LARGE-SCALE ONLINE ENVIRONMENTAL MAPPING: FROM THEORY TO IMPLEMENTATION

A Dissertation by

Ahmad Rabanimotlagh

Master of Science, Wichita State University, 2015

Submitted to the Department of Industrial and Manufacturing Engineering
and the faculty of the Graduate School of
Wichita State University
in partial fulfillment of
the requirements for the degree of
Doctor of Philosophy

December 2017

LARGE-SCALE ONLINE ENVIRONMENTAL MAPPING: FROM THEORY TO IMPLEMENTATION

The following faculty members have examined the final copy of this dissertation for form and content, and recommend that it be accepted in partial fulfillment of the requirement for the degree of Doctor of Philosophy, with a major in Industrial Engineering.

Janet Twomey, Committee Co-Chair

Pu Wang, Committee Co-Chair

Ehsan Salari, Committee Member

Pingfeng Wang, Committee Member

Zheng Chen, Committee Member

Accepted for the College of Engineering

Royce Bowden, Dean

Accepted for the Graduate School

Dennis Livesay, Dean

ACKNOWLEDGEMENTS

I owe my deepest gratitude to my supervisor, Dr. Janet Twomey. I would not have reached this stage without her endless support throughout the long path in my PhD studies. My experiences of working with her are tremendously determining in my entire life.

I am also deeply grateful to my other supervisor, Dr. Pu Wang. This dissertation would not have been completed without his continuous encouragement and support. Besides teaching me to conduct effective research and helping me raise my research skills, he has given me tremendous life visions which I will benefit from throughout my life.

I want to express my sincere thanks to Dr. Ehsan Salari, Dr. Pingfeng Wang and Dr. Zheng Chen for their kind attendance in my dissertation defense committee. Their valuable comments help me improve my research quality remarkably.

I want to appreciate my mother. I would not have had any of my achievements without her endless love and patience.

ABSTRACT

Within the context of environmental studies, environmental mapping addresses the monitoring and analysis of physical processes appearing in the nature, such as atmospheric or oceanic transformations. In such studies, often monitoring is fulfilled by deployment of sensor infrastructures and analytics are legitimized by the existance of statistical models known to represent the unknown nature of the physical process. Despite a great number of researches existing in the field of environmental mapping, development of analytical frameworks that well-utilize the advanced sensor platforms along with theoratically proven novel mathematical ideas to address the existing research gaps is a promising area of effort.

Therefore, the objective of this dissertation is evolved around development of novel frameworks to address the analytical shortcomings of the previous researches in environmental mapping by employing mathematical and statistical techniques on proper sensing platforms. Our proposed frameworks incorporate the stochasticity of the model underlying the physical processes in an online intelligent manner to progressively and adaptively build an accurate representation of the physical process based on modern sensing techonologies in a cost-effective practice. Our research asserts the validity of the proposed frameworks through both theory and implementation.

TABLE OF CONTENTS

TABLE OF CONTENTS (continued)

Chapter **Page**

LIST OF FIGURES

Figure **Page**

CHAPTER 1

INTRODUCTION

Researches in environmental modelling, commonly address the measurement and analysis of physical processes such as underwater pollution concentration, toxic material propagation, ambient air temperature, etc. Environmental modelling generally requires a sampling phase in which measurements of the field under study are taken at limited locations mainly because sampling at all possible locations is impractical and often costly. Environmental mapping is then the problem of field prediction at locations where measurements are unavailable, using geostatistical techniques. Often the outputs of the environmental mapping schemes would be utilized to augment the quality and accuracy of the information given in Geographic Information Systems (GIS) or can be used to construct the field map over the area of study. Environmental mapping is legitimately enabled by the presense of spatially or spatio-temporal(time-varying) distributed models of a random field. However the model used to represent the field may be either stochastic or deterministic. In deterministic models, the model parameters are initially available and known with a high level of accuracy [20]. While with stochastic models, the parameter space is initially unknown, which imposes additional challenges in the geostatistical analyses.

In order to deal with the model parameters uncertainty, conventional methods approach the spatial prediction with parameter identification as an offline procedure. The parameters are first estimated using the available data and then directly plugged into the spatial prediction procedure [22]. This however might lead to underestimated prediction error by undermining the variability in the parameter estimates [15]. On the other hand, online mapping techniques, perform parameter identification and the field spatial prediction as two reflective tasks. An online mapping scheme utilizes the growing knowledge of the field during exploration to improve the accuracy of the parameter identification thereby increase the quality of the spatial prediction in an incremental fashion. The identified pa-

rameters can also incrementally influence the knowledge of the field with incorporating preferential sampling, that is recommending further sampling locations for more accurate representation of the random field.

While static sensor networks have been commonly used for field measurements in mapping schemes with offline paramter identification, exploitation of an online mapping framework demands a different sensing platform. In an online procedure, the base mechanism of sensing should be fast and efficient enough to provide measurements of the required locations in a most cost-effective fashion. In this case static sensor networks are commonly replaced with mobile sensor networks. A mobile sensor network is usually built upon multiple robots equipped with sensors to move around the area and provide samples of the field. This being very appealing and highly practical for large-scale studies, imposes additional challenges of high interrelation between robots configurations (formation and shape) and mapping, which will be elaborated in chapter 4.

Given the above limitations existing in the literature, development of proper environmental mapping systems for accurate representation of the fields is linked with appropriate incorporation of parameters uncertainty in the model and deployment of efficient sensing platforms. Thus, in this disseration, we will propose two schemes for large-scale online environmental modeling of scalar random fields with uncertain spatial models, aimed to utilize cost-effective sensing platforms for field sampling. Within the proposed schemes, we address the problems of parameter identification and spatial prediction in a real-time and environmental adaptive fashion. This besides providing a model of a high accuracy also increases the quality of the constructed field map.

1.1 Research Scope and Objectives

In this dissertation, we propose two novel schemes for large-scale online environmental modeling. Our frameworks are generic and can be applied for the scenarios of the random field with underlying spatial or spatial-temporal Gaussian processes. We will evaluate the performance of our frameworks based on three different applications.

In the first framework, we address the static environmental modeling where the random field at different locations is spatially correlated. We develop an iterative Bayesian decision scheme for spectrum mapping and TV white space (TVWS) discovery. TVWS represents the underutilized TV spectrum at a particular frequency bandwidth which can be used for white space devices (WSD) communications without interference with the primary users communicating on that particular bandwidth. On the data collection aspect, we propose a prototyped portable device designed for cost-effective signal power sensing. On the problem formulation aspect, we consider a stochastic spatially distributed model of spectrum power where the parameter identification and field map construction is performed iteratively. We propose a Bayesian decision framework which coherently combines Bayesian spatial prediction and Bayesian experimental design with an objective to optimally select mobile users as well as their locations to achieve the desired accuracy of the spectrum map. This frameowrk is aimed to be deployed in a cloud-based crowd-augmented spectrum mapping system, where WSD users contribute to the task of sensing. The measurements of the field taken by WSD users can be sent to a centralized remote server where the computations are performed. If the desired level of mapping accuracy is not met using the data collected so far, additional locations for sampling are selected and the process continues with further sampling by WSD users. In fact, crowd sourcing of WSD users for field measurement facilitate a very cost-effective way of field sampling at various locations in an agile and efficient manner. The proposed schemes will be implemented for TVWS detection for the Wichita State University main campus as the area of study.

In the second framework, we address the dynamic environmental modeling where the random field at different locations is spatially and temporally correlated. A joint sensing-motion-mapping scheme is proposed, designed for a mobile sensor network system. A swarm of robots can move around the area of interest, take the field measurements, perform parameter identification and construction of the field map in a real-time, cooperative

and adaptive fashion. In this case, the model and prediction accuracy is strongly linked with parameter identification as well as formation and trajectory of the robots for sampling. Within our proposed procedure, the growing information of the field during exploration is utilized to perform robust parameter identification and also control the formation and trajectory of the agents for an environmental adaptive field exploration. The performance of the proposed framework is evaluated with simulations based on two different applications. First, an underwater acoustic communication channel is considered with a system of a linear time-varying impulse response with the channel gain as the spatial-temporally correlated random field. Second, the advection-diffusion field is considered, which has been widely adopted to characterize the propagation of many physical processes in nature in particular atmospheric and waterborne pollution.

1.2 Dissertation Proposal Organization

The rest of this dissertation is organized as follows. In chapter 2, we provide a brief literature review of the researches in environmental mapping. In chapter 3, we introduce an iterative Bayesian decision framework for optimal spectrum mapping. In chapter 4, we describe a cooperative field exploration scheme for mobile sensor networks. The simulated environments to evaluate the performance of the framework introduced in chapter 4 are described in chapter 5. Conclusion of our research is given in chapter 6 and directions of future research are described.

CHAPTER 2

LITERATURE REVIEW AND RESEARCH MOTIVATION

Researches in environmental modeling have evolved broadly covering atmospheric, terrestrial and underwater environments. Here, we present a brief review of the literature as related to our application, i.e. spectrum mapping and TVWS discovery, environmental modeling with mobile sensor networks.

2.1 Terrestrial Channel Modeling

Digital TV broadcasting in united states has been identified by FCC as one of the underutilized spectrum bands and henceforth made open to unlicensed users under the condition of no interference with licensed user communications. To identify the possible interference, regulators (e.g., FCC, Ofcom, ECC) offer spectrum database providers who maintain the spectrum availability information for every location. Unlicensed user have to contact one of the authorized white space database providers to know the spectrum availability information for their intended location before initiating the communications. Recently, large-scale spectrum measurements (in Hong Kong [57] and New York [7]) have shown that geo-location databases, as the recommended approach by regulators [36] for TVWS discovery are notoriously inaccurate in Metropolitan areas. For example, the spectrum availability information in such databases is based on the TV transmission specifications of broadcaster and their coverage might be modeled using FCC 66602 model. This model predicts TV tower coverage area in a gradient descent manner which does not consider the signal degradation under small-scale fading effects, such as reflection and refraction. Though such factors are ineffective at locations near the TV transmission tower but they have shown to mislead the database information in locations with long distances from transmission tower. To resolve this issue and achieve maximum accuracy in white space spectrum discovery, it is essential to build a spectrum database which is purely based on spectrum sensing measurements. The spectrum sensing measurements

can then serve as the input to a spectrum mapping scheme with the objective of TVWS discovery.

The objective of spectrum mapping is to create a power spectrum density (PSD) map for an area of interest, where each location on the map is associated with its corresponding PSD value. If the PSD value at a location is smaller than a preset threshold (-114 dBm for digital TV service), then the TV channel is considered as white. Apparently, sampling PSD at every location is impractical and cost-consuming. Towards this, geostatistical methods can be applied for spectrum mapping. By such methods, PSD is only sampled at a limited number of locations, and the measurements at these locations are utilized to predict the PSD value at any other non-sampling locations.

The measurement-augmented geo-location databases have been recently proposed, which rely on the refined propagation model, whose accuracy is improved by the spectrum sensing measurements collected by dedicated vehicles [7] or public transmit systems (e.g., Buses) [61] which are equipped with spectrum sensing devices. However, those geo-location databases still face fundamental limitations. Their performance enhancement is relying on the measurements from the spectrum sensing vehicles, which can only travel to a limited number of locations. Thus, it will be cost prohibitive for them to provide the high spatial-resolution spectrum map covering the entire area in large-scale outdoor or indoor environments. Limitations of all the existing geostatistical spectrum mapping schemes,[40, 52, 56, 49, 51] can also be described in two additional fundamental issues:

Predictor design with accurate error assessment: Before spectrum mapping is conducted, all the parameters of the underlying spatial model are unknown. To counter this problem, all the existing spectrum mapping schemes adopt the classical two-phase kriging predictor from geostatistics, where the parameter estimation and the PSD prediction are operated separately and sequentially. This means that the unknown parameters are first estimated by fitting the parametric covariance function to an empirical variogram,

and then the estimated parameter values are plugged into theoretical kriging prediction equations as if these estimated parameter values were the true values [15]. It has been established in geostatistics that the two-phase kriging leads to optimistic assessments of predictive accuracy in the sense that it underestimates prediction error by ignoring variability between parameter estimates and their true, unknown values [15]. Speaking of spectrum mapping, such underestimated prediction error implies the increased probability of mis-detection.

Optimal user selection with unobserved future data: So far, all the existing geostatistical spectrum mapping solutions deal with the *retrospective design problem*, where a design or action is to be chosen after the data are collected. Regarding spectrum mapping, it means that a dense network of monitoring locations is established and data are collected from each location. Armed with the data from these monitoring locations, an efficient predictor is developed to build the spectrum map with the minimum global prediction error. On the contrary, our crowd-augmented spectrum mapping scheme deals with *prospective design problem*, which means that we do not know in advance what measurements the mobile users will contribute, before actually selecting them to perform PSD sampling. Therefore, we have to predictively select the optimal mobile users who expectedly have the most useful sampling data, such that accurate and high-resolution spectrum map can be built.

In our research, towards the optimal cloud-based crowd-augmented spectrum mapping, we will address two problems: (1) the implementation of a theoretically optimal predictor to minimize the local predication error at non-sampling locations, and (2) the design of optimal user selection scheme to find the appropriate locations for sampling by mobile users so that the desired global predication error is met. To simultaneously address the above two challenges, we propose a iterative Bayesian decision framework, which coherently combines Bayesian spatial prediction and Bayesian experimental design. *Bayesian spatial prediction* will be exploited to address the limitations of the two-

phase kriging scheme by implementing the optimal predictor, whose prediction error can be accurately assessed. More specifically, Bayesian spatial prediction treats unknown parameters as random variables, and therefore makes no formal distinction between parameter estimation problems and prediction problems [13]. This provides a natural means of allowing for parameter uncertainty in predictive inference for the PSD at non-sampling locations, which leads to a much more honest and accurate assessment of prediction error. Moreover, Bayesian spatial prediction aims to derive the predictive distribution at non-sampling locations, therefore providing a nature way to implement the optimal predictor. *Bayesian experimental design* will be utilized to optimally select the additional mobile users for sampling under the uncertainty caused by unobserved future data and unknown parameters [8]. Bayesian experimental design, which is widely applied in bioinformatics, is concerned with making the optimal decisions to maximize the expected utility, i.e., utility averaged over all possible outcomes of a decision before data are collected. In our case, assisted by Bayesian spatial prediction, the utility function will be designed to accurately reflect the quality improvement of the spectrum map, e.g., the global prediction error reduction.

2.2 Mobile Sensor Networks

There are numerous researches evolved around utilizing mobile sensor networks for environmental modeling. A mobile sensor network is basically a swarm of robots equipped with sensors moving around an area to take measurements of the field at different locations. The growing information during field exploration can be exploited incrementally for field map reconstruction in a real-time, cooperative and environmental-adaptive fashion. Here, our research is focused on the application of mobile sensor networks for the exploration of random fields characterized by Gaussian processes (GP) based on the reduced dimention Kriged Kalman filter (KKF) model [54]. Kriged Kalman filter has been well discussed in [34] and [12] and utilized vastly in numerous researches for scalar random field exploration [26], [11], [20], [29], [28], [9] and [10].

The use of mobile sensor networks is highly appealing in terms of sampling efficiency and envionmental adaptability. However, significant challenges with the use of mobile sensor networks are imposed, as pertaining to model and mapping accuracy with respect to the measurements becoming available over time. This implies the necessity of the presence of a methodology to well-utilize limited amount of measurements which are often noise-corrupted and adaptively include the growing information during exploration. Cortes [11] has introduced a distributed framework for exploration of scalar random fields using Kriged Kalman filter (KKF) model. With random field assumed to be spatio-temporally distributed, a novel framework for mobile sensor networks has been introduced in which the random field predictive mean and variance are effectively estimated through a distributed average weighted least squares method. La and Sheng [29] have introduced a framework for data fusion for scalar field mapping in a mobile sensor network where each agent has the capability of measuring the field value at its own locations and surrounding near locations. The spatio-temporal properties of the random field are assessed using three consensus filters. A flocking-control path planning strategy is introduced for the mobile sensor network, which controls for the formation, navigation and damping force. Kim et al. [26] have utilized the dimention-reduced KKF model in a cognitive radio application for channel gain mapping. Atanasov et. al [4] have considered a model-free and a model-based approach for the source-seeking application. In their model-free approach, the mobile sensor network is guided towards the areas with high levels of signal field based on the gradient of the random field at the centroid of the network, evaluated through finite-difference approximation. In their model-based approach, the path planning strategy is based on the mutual information of the signal and measruement process. The distributed version of both approaches have been also presented. Singh et. al [46] have proposed an efficent path planning strategy fo robotic systems under spatiotemporally correlated fields. Their approach includes the methods to update the covariance function in an incremental fashion after each round of new observations. Guestrin et. al [21] have

proposed a computational complexity-reduced greedy heuristic for sampling design, such that the sampling locations are selected sequentially to maximize the increase in mutual information after adding each location. Choi et. al [10] presented a cooperative learning framework for unknown field exploration using a group of autonomous agents where each agent progressively builds a map of the field using its own data and those received from neighbor agents. In a different research, Choi et. al [9] considered KKF model for a scalar random field explored by a mobile sensor network. They controlled the navigation of each individual robot by combining different path planning strategies into a single control.

Another complexity rising with the use of mobile sensor networks for field exploration is the effect of network formation and trajectory on the mapping accuracy. The performance of a mapping scheme utilized in a mobile sensor network is highy depended on the sampling locations. This needs an intelligent mechanism during exploration to provide the agents on recommended sampling locations in the form of formation shape and trajectory. Coopearative strategies have been adopted in the literature to be utilized on mobile sensor network platforms, [38] [32] [59] [60] to name afew. In [60], the cooperative exploration problem has been defined as minimizing the error in estimation of the field values given the statistics on the model parameters by simultaneous cooperative motion and filtering.

In this research, towards scalar random field exploration with mobile sensor networks, we develop a KKF model linked with the formation of the robots. This is a unique feature that is utilized to optimize the formation of the robots during exploration in an environmental adaptive fashion. Parameter identification is performed in an online fashion by recursively utilizing the information obtained during exploration within a slide-window. The network trajectory is planned such that robots move along the information-rich paths so that the mapping error is minimized effectively in an iterative fashion. The proposed framework can be used for field exploration in multiple settings including terrestrial, underwater or atmospheric environments for scalar random field mapping. It can also be

easily extended for applications other than mapping such as source seeking, level-curve tracking, etc.

CHAPTER 3

OPTIMAL CROWD-AUGMENTED SPECTRUM MAPPING VIA AN ITERATIVE BAYESIAN DECISION FRAMEWORK

In this chapter, we present an iterative Bayesian decision framework which aims to construct an accurate representation of the spectrum map of a geographical area over multiple PSD sampling rounds. Relying on two major components of *Bayesian spatial prediction* and *Bayesian experimental design*, our framework addresses two fundamental problems: (1) the implementation of a theoretically optimal predictor to minimize the local predication error at all non-sampling locations, and (2) the design of optimal user selection scheme to determine the mobile users with appropriate locations for additional sampling so that the desired global predication error is met. Bayesian spatial prediction is utilized to address the limitations of the two-phase kriging scheme by implementing the optimal predictor, whose prediction error can be accurately assessed. More specifically, Bayesian spatial prediction treats unknown parameters as random variables, and therefore makes no formal distinction between parameter estimation problems and prediction problems [13]. This provides a natural means of allowing for parameter uncertainty in predictive inference for the PSD at non-sampling locations, which leads to a much more honest and accurate assessment of prediction error. Moreover, Bayesian spatial prediction aims to derive the predictive distribution at non-sampling locations, therefore providing a nature way to implement the optimal predictor. Bayesian experimental design is utilized to optimally select the additional mobile users for sampling under the uncertainty caused by unobserved future data and unknown parameters [8]. Bayesian experimental design, which is widely applied in bioinformatics, is concerned with making the optimal decisions to maximize the expected utility, i.e., utility averaged over all possible outcomes of a decision before data are collected. In our case, assisted by Bayesian spatial prediction, the

utility function is designed to accurately reflect the quality improvement of the spectrum map, e.g., the global prediction error reduction.

3.1 Overview of Optimal Crowd Augmented Spectrum Mapping

Consider an area of interest $\mathcal{A} \in \mathbb{R}^2$, where the PSD can be modeled as a Gaussian random field $\mathbf{S} = (S(x) : x \in \mathcal{A})$, where $S(x)$ indicates the PSD value at location x with mean $E[\mathbf{S}] = \mu$ and variance $Var[\mathbf{S}] = \sigma^2$. Such model has been verified through both experimental and theoretical analysis [50][42][1][27][6] and has been widely adopted to characterize the random attenuation (in dBm) caused by flat fading. After sampling the PSD at certain locations, the PSD measurements (in dBm) are of the form $(x_i, y_i) : i = 1, ..., n$, where $\mathbf{x} = \{x_1, ..., x_n\}$ are sampling locations within the area $\mathcal{A}$, and $\mathbf{y} = \{y_1, ..., y_n\}$ are the PSD measurements at these locations. As a result, **y** can be considered as a realization of measurement process **Y**, where $\mathbf{Y} = (Y(x) : x \in \mathcal{A})$ is the noisy versions of the signal process **S** (PSD field), i.e.,

$$Y(x) = S(x) + N \tag{3.1}$$

where N is the background noise with zero mean $E[N] = 0$ and variance $Var[N] = \tau^2$

The feasibility of geostatistical methods for spectrum mapping rely on the fact that PSD measurements are spatially correlated, i.e., the PSD values at adjacent locations trend to be similar. More specifically, the spatial correlation between any two locations x_i and x_j is a function of their euclidean distance $d_{ij} = ||x_i - x_j||$ and is defined as

$$\rho(d_{ij}; \phi) = \frac{Cov(S(x_i), S(x_j))}{\sigma^2} = \frac{E[(S(x_i) - \mu)(S(x_j) - \mu)]}{\sigma^2} \tag{3.2}$$

where $E[S] = \mu$ and $Var[S] = \sigma^2$ are the mean and variance of the random field S. The spatial correlation model $\rho(d; \phi)$ may depend on one or more parameters denoted by vector ϕ. For example, $\phi = \bar{d}$ for exponential correlation model $\rho(d; \{\bar{d}\}) = e^{-(d/\bar{d})}$, and $\phi = (\bar{d}, k)$ for power exponential correlation model $\rho(d; \{\bar{d}, k\}) = e^{-(d/\bar{d})^k}$. Both models have been experimentally verified to characterize the spatial correlation under the impact of shadowing [50].

Given the measured PSD **y** at sampling locations, the predictor of PSD $S(x)$ at any non-sampling location x is denoted by $\hat{S}(x)$, which is a function of measurement **y**, i.e., $\hat{S}(x) = g(\mathbf{y})$. The performance of the predictor can be characterized by its mean squared predication error $E[(\hat{S}(x) - S(x))^2]$ and its biasedness $E[\hat{S}(x) - S(x))]$. The optimal predictor is the conditional mean predictor, i.e.,

$$\hat{S}_{opt}(x) = E[S(x)|\mathbf{Y} = \mathbf{y}] \tag{3.3}$$

which is unbiased, i.e., $E[\hat{S}(x) - S(x)] = 0$ and has the minimum mean squared predication error among all possible predictors

$$PE_{opt}(x) = E[(\hat{S}_{opt}(x) - S(x))^2] = \min(E[(\hat{S}(x) - S(x))^2]) \tag{3.4}$$

It follows by spatial statistical analysis that $PE_{opt}(x)$ is a function of (1) random field variance σ^2, (2) the $n \times n$ spatial correlation matrix **R** with $(i,j)^{th}$ element $\rho(||x_i - x_j||; \theta)$, and (3) the spatial correlation vector **r** with element $r_i = \rho(||x_0 - x_i||; \theta)$, where $i = 1, ..., n$. Therefore, the sampling locations directly determine the prediction error at non-sampling locations, thus impacting the accuracy of the spectrum map.

To achieve the desired level of accuracy in spectrum mapping, the locations of mobile users for spectrum sensing has to be controlled. Towards this, our optimal crowd-augmented spectrum mapping aims to answers the fundamental question of which mobile users should be selected to measure PSD, such that the optimal predictor can be realized, while ensuring that the global prediction error is smaller than a predefined threshold, $GPE_{\mathcal{A}} < GPE_{th}$. In particular, the global prediction error is defined as the spatial average predication error $GPE_{\mathcal{A}}$ over the area $\mathcal{A}$,

$$GPE_{\mathcal{A}} = \frac{1}{|\mathcal{A}|} \int_{\mathcal{A}} PE_{opt}(x) dx \tag{3.5}$$

3.2 Iterative Bayesian Decision Framework

The key mechanism of our proposed framework is to progressively improve spectrum mapping performance in multiple iterations, as shown in Fig. 3.1. The proposed

framework includes the iterative operations of MCMC-assisted Bayesian spatial prediction, expected utility evaluation, and utility-optimal Genetic Algorithm (GA) for mobile user selection. At the first iteration, the PSD measurements are available at relatively spare locations. Based on such limited information, there will exist significant uncertainty in the parameter estimations and high prediction error in the PSD values at the non-sampling locations. In the following iterations, additional sets of mobile users, which are expected to decrease the global prediction error, will be selected to report the PSD measurements. The accumulation of additional measurements from the previous rounds not only help to gain more knowledge about the experiment, such as the expected utility or gain of different user selection choices, but also help to reduce the uncertainty in the unknown parameters and the randomness in the predicted PSD values.

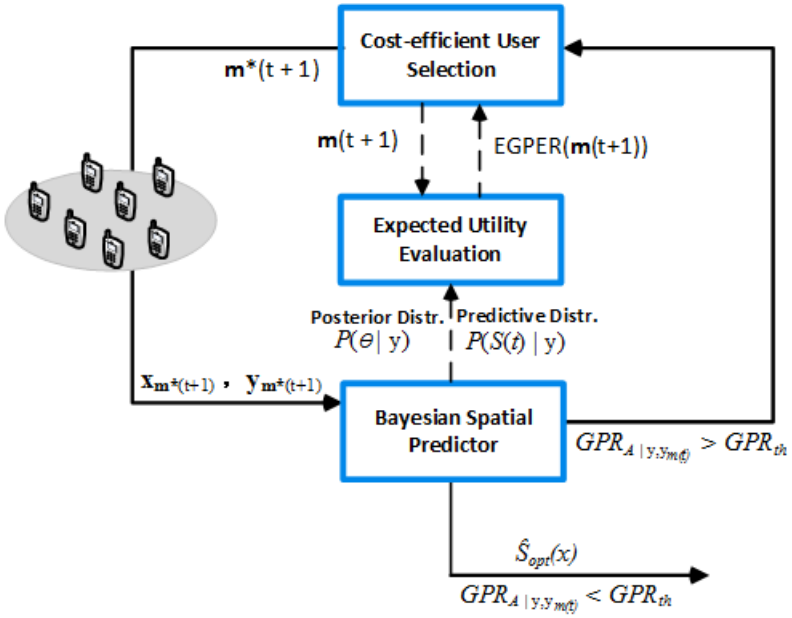

Figure 3.1: Iterative Bayesian decision framework

3.2.1 MCMC-assisted Bayesian spatial prediction (Step 1):

Initially, all the parameters of the random field **S** are unknown, which are represented by the vector

$$\theta = (\mu, \sigma^2, \phi, \tau^2) \tag{3.6}$$

Following Bayesian spatial prediction principle, unknown parameters θ are treated as random variables assigned with arbitrary prior parameter distributions $P(\theta)$, such as uniform, Gamma, and Gaussian distributions. It is known that as the measurements **y** are growing, the posterior distribution will be concentrated around the maximum likelihood estimate and is insensitive to the choice of prior distributions. After obtaining the measurements **y** from mobile users, the posterior parameter distribution, $P(\theta \mid \mathbf{y})$ is computed by Bayes' rule as follows:

$$P(\theta \mid \mathbf{y}) \propto P(\mathbf{y} \mid \theta)P(\theta) \tag{3.7}$$

where by spatial statistics in Gaussian random field **S**, $P(\mathbf{y} \mid \theta)$ follows multivariate Gaussian distribution with mean and covariance matrix as the function of θ. By $P(\theta \mid \mathbf{y})$, we can obtain the Bayesian spatial predictor of $S(x)$, which is the optimal predictor as shown in (3.3), by:

$$\hat{S}_{opt}(x) = E(S(x) \mid \mathbf{y}) = \int P(S(x) \mid \theta, \mathbf{y})P(\theta \mid \mathbf{y})d\theta \tag{3.8}$$

where $[S(x) \mid \theta, \mathbf{y}]$ follows a Gaussian distribution [15] with mean and variance as:

$$E[S(x) \mid \theta, \mathbf{y}] = \mu + r'V(\theta)^{-1}(Y - \mu) \tag{3.9}$$

and

$$Var[S(x) \mid \theta, \mathbf{y}] = \sigma^2(1 - r'V(\theta)^{-1}r) \tag{3.10}$$

Finally, the prediction error at location x, $PE_{opt}(x \mid \mathbf{y})$, and the global predication error over the whole area $\mathcal{A}$, $GPE_{\mathcal{A} \mid \mathbf{y}}$, can be obtained by evaluating the conditional variance given observations **y**:

$$PE_{opt}(S(x) \mid \mathbf{y}) = \int Var[S(x) \mid \theta, \mathbf{y}]P(\theta \mid \mathbf{y})d\theta \tag{3.11}$$

and

$$GPE_{\mathcal{A} \mid \mathbf{y}} = \frac{1}{|\mathcal{A}|}\int_{\mathcal{A}} PE_{opt}(S(x) \mid \mathbf{y})dx \tag{3.12}$$

For Bayesian spatial predictor, its prediction error $PE_{opt}(x)$ seamlessly incorporates $P(\theta \mid \mathbf{y})$ which describes the uncertainty of the parameter estimations. This leads

to a much more accurate assessment of the prediction error compared to conventional Kriging algorithm. To implement Bayesian spatial predictor, we need to deal with the analytically intractable poseterior distribution and integrals. Towards this, Markov chain Monte Carlo (MCMC) methods will be applied to generate samples from the posterior predictive distribution $P(S(x)|\mathbf{y})$ and posterior parameter distribution $P(\theta|\mathbf{y})$ both of which may follow analytically intractable and arbitrarily complex methods. By strong Law of Large Numbers and sample mean calculation, these MCMC simulated samples will be used to numerically compute the Bayesian spatiial prediction $\hat{S}_{opt}(x)$ in (3.8) and its prediction error $PE_{opt}(S(x) \mid \mathbf{y})$ in (3.11). The implementaiton details are given in section IV (B).

3.2.2 Expected Utility Evaluation (Step 2):

Based on the measurements already taken, if the global prediction error is larger than the desired threshold, i.e., $GPE_{\mathcal{A} \mid \mathbf{y}} > GPE_{th}$, additional mobile users will be selected to augment the current spectrum map. At t-th round, let $\mathbf{m}(t)$ denote a set of mobile users appearing at locations $\mathbf{x}_{m(t)}$ with PSD measurements $\mathbf{y}_{m(t)}$, i.e., $\mathbf{m}(t) = (\mathbf{x}_{m(t)}, \mathbf{y}_{m(t)})$. Since our objective is to improve global prediction accuracy, we will define the global prediction error reduction (GPER) as the utility or gain of selecting mobile users $\mathbf{m}(t)$, i.e.

$$GPER(\mathbf{m}(t)) = \int_{\mathcal{A}} \big(Var[S(x) \mid \theta, \mathbf{y}] - Var[S(x) \mid \theta, \mathbf{y}, \mathbf{y}_{m(t)}]\big) dx \tag{3.13}$$

Because the parameter vector θ is unknown and $\mathbf{y}_m$ are yet unobserved future data, we need to adopt expected utility function

$$EGPER(\mathbf{m}(t)) = \int GPER(\mathbf{y}_{m(t)}) P(\mathbf{y}_{m(t)} \mid \mathbf{y}, \theta) P(\theta \mid \mathbf{y}) d\theta d\mathbf{y}_{m(t)} \tag{3.14}$$

which is the expected global prediction error reduction (EGPER) of selecting the mobile users $\mathbf{m}(t)$, marginalizing over the predictive distribution of observations $\mathbf{y}_{m(t)}$ and the posterior distribution of the unknown parameter vector θ. It is worth to note from the optimal prediction theory that with the optimal predictor, the conditional variance $Var[S(x) \mid \theta, \mathbf{y}]$

only depends on the locations **x** of observations **y** instead of their values. This means $GPER(\mathbf{m}(t)) = GPER(\mathbf{x}_{m(t)})$ and

$$EGPER(\mathbf{m}(t)) = EGPER(\mathbf{x}_{m(t)}) = \int GPER(\mathbf{x}_{m(t)}) P(\theta \mid \mathbf{y}) d\theta \tag{3.15}$$

This feature avoids evaluating all possible values of $\mathbf{y}_{\mathbf{m}(t)}$, when computing the expected utility $EGPER(\mathbf{m}(t))$. This greatly reduces the computational cost involved for expected utility evaluation.

3.2.3 Expected-utility optimal GA for cost-effective user selection (Step 3):

After obtaining the measurements from $\mathbf{m}(t)$ mobile users at the t-th round, if the global prediction error is still larger than the desired threshold, i.e., $GPE_{\mathcal{A} \mid \mathbf{y}, \mathbf{y}_{m(t)}} > GPE_{th}$, then another set of mobile users $\mathbf{m}(t+1)$ will be selected at the $t+1$-th round. Intuitively, at each round, we should select the users that leads to the maximum expected global prediction error reduction (EGPER). By such way, a small number of rounds is expected to reach the desired global prediction error. As a result, the total number of selected mobile users can be greatly reduced. Towards this, we will develop the expected-utility optimal algorithm for cost-effective user selection. First, we set N as the number of users to be selected at each round and then choose the set of $\mathbf{m}^*(t+1)$ users that can maximize the EGPER, i.e.,

$$\mathbf{m}^*(t+1) = \arg\max_{\mathbf{m}(t+1)} EGPER(\mathbf{m}(t+1)) \tag{3.16}$$

As mentioned in (3.15) of step 2, the evaluation of EGPER only needs the location information of to-be-selected users. Thus, solving the optimization problem in (3.16) is equivalent to finding the optimal spatial configuration or subset of locations, $\mathbf{x}^*_{t+1} \subset \mathbf{x}^{\mathcal{A}}_{t+1} : |\mathbf{x}^*_{t+1}| = N$, in such a way that

$$\mathbf{x}_{m^*(t+1)} = \mathbf{x}^*_{t+1} = \arg\max_{\mathbf{x}^*_{t+1} \subset \mathbf{x}^{\mathcal{A}}_{t+1} : |\mathbf{x}^*_{t+1}| = N} EGPER(\mathbf{x}_{t+1}) \tag{3.17}$$

where $\mathbf{x}_{(t+1)}$ are the locations of all mobile users in area $\mathcal{A}$ at round $t+1$.

However depending on the number of potential locations for additional sampling, the exhaustive search of the entire solution space to find the locations for maximum expected utility would be extremely costly. Towards this, we will develop a Genetic Algorithm (GA) which can be utilized to efficiently search the solution space. As a population-based search method inspired by biological evoultion, GA has been thus far applied widely for evolutionary computations in veriety of applications. They have been experimentally providing good solutions for the problems of very little information [35] [5]. The implementation details are given in section IV (C).

3.3 Implementation Details

3.3.1 Spectrum Sensing Device Prototype

Due to unavailability of a commercial white space device (WSD) for spectrum sensing, we prototype a portable device for this purpose. Fig. 3.2 shows our spectrum sensing device where B200mini acts as the radio front-end and tunes the receiver on the desired TV channel. ANT 500 is connected to USRP B200mini for improvement on the receiver signal detection. Raspberry Pi 2 as a low power computing platform running on Linux Operating System, is equipped with GNURadio software package for radio frequency (RF) signal processing. We calibrated our mobile spectrum sensing device by tuning the parameters to ensure that the measurements are consistent with the keysight N9322C spectrum analyzer information for some random locations.

The key idea of our spectrum sensing algorithm is to detect the presence of the pilot signal in every 6 MHz TV channel by determining its PSD and then estimate the PSD of the entire TV channel based on the PSD of the pilot singal. In particular, according to the ATSC digital TV standard adopted in United States, the pilot signal is transmitted at 310KHz above the lower band of TV channel frequency. Moreover, ATSC pilot contributes 0.3 dB of the total signal power, which makes it 11.45dBm lower than the PSD of whole channel. For instance, if the PSD of the pilot signal is -120 dBm, this means that PSD of the TV channel over the entire 6 MHz is -108.55 dBm.The spectrum sensing module is

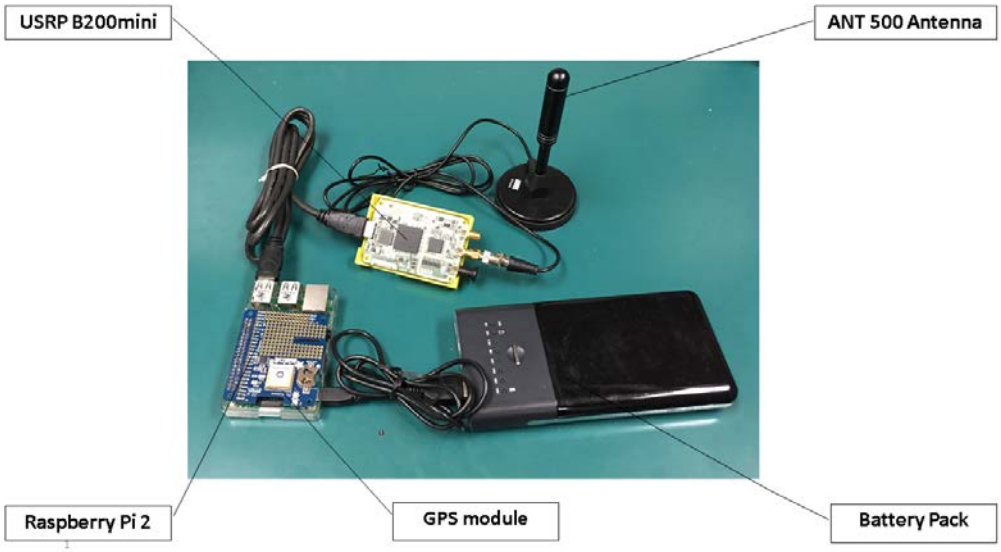

Figure 3.2: Spectrum sensing device prototype

implemented using GNURadio libraries, which performs fast fourier transform (FFT) operation to calculate the PSD value. External GPS antenna is used to identify the location coordinates when each measurement is taken. The sensing platform is connected to a custom created spectrum database. The spectrum sensor platforms upload the location information and the received PSD of the channel to the spectrum database once entering the coverage area of the intended research Wi-Fi network.

3.3.2 Parameter and Signal Sampling based on Metropolis-Hastings procedure

In order to implement the proposed framework, the region $\mathcal{A}$ is descretized into a grid with prespecified distances. The set of all points in the grid represents the prediction locations, $\mathbf{x}^p$. The core components of this implementation include parameter sampling and signal sampling schemes. The objective of parameter sampling is to numerically approximate the posterior distribution of the parameters, Eq. (3.7), which is required to compute the Bayesian spatial prediction error, Eq. (3.12). The signal sampling scheme is used to obtain a numerical approximate of the posterior predictive distribution, which along with the parameter samples are required in computation of the Bayesian spatial prediction,

Eq. (3.8). To deal with the analytically intractable and complex posterior distribution and integrals, Markov Chain Monte Carlo (MCMC) methods are applied. The basic idea of MCMC methods is that, when independent sampling from a complex non-standard stochastic process, say P, is impractical, large-scale dependent sampling from a Markov chain, which has P as its equilibrium distribution, would provide reliable samples [17] [47] [19]. The Monte Carlo integration can then use the Markov chain generated samples to estimate the statistics of P.

Let $GPE_{\mathbf{x}^p}$ and $BSP_{\mathbf{x}^p}$ denote the global prediction error and Bayesian spatial prediction over all prediction locations respectively. Algorithm 1 represents the overall procedure of the proposed framework. Initially, starting with the existing PSD measurements at relatively sparse location, parameter sampling is performed and $GPE_{\mathbf{x}^p}$ is in turn computed. The procedure of additional PSD measurements, parameter sampling and re-evaluating the global prediction error is continued until the termination criteria is met, i.e., the global prediction error is smaller than the desired threshold, i.e., $GPE_{\mathbf{x}^p} < GPE_{th}$. At this stage, signal sampling is performed, $BSP_{\mathbf{x}^p}$ is computed and PSD field heatmap is constructed.

Algorithm 1 Iterative Bayesian decision framework

```
1: procedure FIELDMAPCONSTRUCTION
2:     while termination criteria is not met do
3:         take parameter samples (Algorithm 2)
4:         compute GPE_{x^p}, i.e., Eq. (3.12)
5:         if termination criteria is met then
6:             take signal samples
7:             compute BSP_{x^p}, i.e., Eq. (3.8)
8:             generate the spectrum map
9:             break
10:        end if
11:        compute Eq. (3.17) to select the optimal
12:        locations for PSD measurements
13:        (Algorithm 3)
14:    end while
15: end procedure
```

To realize parameter and signal sampling, we apply block-wise Metropolis-Hastings (MH) algorithm, which is one of the MCMC methods [14]. Algorithm 2 represents our MH-based parameter sampling scheme and the signal sampling follows the similar procedure, which is omitted here. In particular, the parameter sampling is initialized with assignment of legitimate values to the unknown parameters considering their prior distributions and computation of the posterior parameter distribution density value based on the initial sample (lines 2-3). The parameter sampling procedure is then continued iteratively. At each iteration t, an additional sample θ^p is proposed for the parameters based on the proposal distribution q and the previous parameter sample $\theta^{(t-1)}$ (line 5). Then the probability of accepting the proposed parameter sample is computed based on the posterior parameter distribution in the current and previous iterations as well as the probability of transition of the Markov chain from the state in previous iteration to the newly proposed state and vice versa (line 6). A uniformly distributed random number is then generated and the proposed sample is either accepted or rejected accordingly (lines 7-12). The MH sampling procedure in Algorithm 2 is also equipped with burn-in and thinning features to draw samples of higher reliabilities. Burn-in implies on discarding a number of initial samples to decrease the dependency of the samples on the starting state. Thining indicates memorizing the generated samples based on a particular time-step in order to reduce the dependence between consecutive samples.

3.3.3 Elitism-based Binary Genetic Algorithm for cost-effective user selection

To find the locations for additional sampling, application of the discrete optimization algorithms to find the optimal subset of locations among the locations in the grid, is a practical approach. However, finding the optimal subset of locations for additional sampling in the discrete space, (i.e., solving the optimization problem in Eq. (3.17)), is still NP-hard. In order to tackle this challenge, we develope a GA to find a good solution for the problem in a time-effective manner. Compared to other metaheuristic algorithms such as Particle Swarm Optimization (PSO) or Simulated Annealing (SA), GAs have been dominantly

Algorithm 2 MH-based parameter sampling

procedure PARAMETERSAMPLING
  $\theta^{(0)} \leftarrow (\mu^{(0)}, \sigma^{2(0)}, \phi^{(0)}, \tau^{2(0)})$
  $P(\theta^{(0)}|y) \leftarrow P(y|\theta^{(0)})P(\theta^{(0)})$
  for number of parameter sampling iterations **do**
    $\theta^{p} \sim q(\theta|\theta^{(t-1)})$
    $\Delta(\theta^{(t-1)}, \theta^{p}) \leftarrow min\{1, \frac{P(\theta^{p}|y)q(\theta^{(t-1)}|\theta^{p})}{P(\theta^{(t-1)}|y)q(\theta^{p}|\theta^{(t-1)})}\}$
    $rand \sim U[0,1]$
    if $rand < \Delta(\theta^{(t-1)}, \theta^{p})$ **then**
      $\theta^{(t)} \leftarrow \theta^{p}$
    else
      $\theta^{(t)} \leftarrow \theta^{(t-1)}$
    end if
  end for
end procedure

used to solve a veriety of combinatorial optimization problems. GA is a polulation-based optimization algorithm where a population consists of multiple chromosomes and each chromosome represents a feasible solution to the problem. In this case, we encode a chromosome as a binary array with each element taking 0 or 1 to represent an unselected or a selected location respectively. This size of this array is equal to the total number of candidate locations for additional sampling. To generate feasible solutions for the problem and avoid violating the assumption of fixed number of additional locations in the Genetic optimization process, the crossover and mutation operations introduced in the Genetic Fix Algorithm [37], are adopted. Let nes denote the number of elite solutions to preserve at each iteration of the GA. Algorithm 4 demonstrates our customized elitism-based binary GA for mobile user selection.

3.4 Experimental Verification

The proposed spectrum mapping framework is verified on our University main campus as the area of study. TV Channel 15 is chosen as the target spectrum bandwidth because the base station of Channel 15 is close to the campus (Fig. 3.3 from Im-

Algorithm 3 Elitism-based GA for additional mobile user selection

procedure USERSELECTION
    The first population, $pop^{(0)}$, is initialized randomly
    $t \leftarrow 1$
    while maximum number of iterations is not reached **do**
        Compute the fitness value $EGPER$ (Eq. (3.15)) for each chromosome (i.e., a set of locations) in the last population based on the parameter samples taken in Algorithm 2.
        Move the top nes chromosomes with the larger fitness values (i.e., the larger $EGPER$ values) from the last population to the current population, $pop^{(t)}$
        Randomly select chromosomes from the last population using fitness-based roulette wheel selection for cross-over operation
        Perform mutation operation on the chromosomes resulted from the crossover operation.
        Add the resulting chromosomes to the current population, $pop^{(t)}$
        $t \leftarrow t + 1$
    end whilereturn the chromosome with the largest fitness value found, i.e., the optimal set of locations with the largest $EGPER$ value.
end procedure

agery, Google, Map data) and is not available (or "white") according to Google spectrum database.

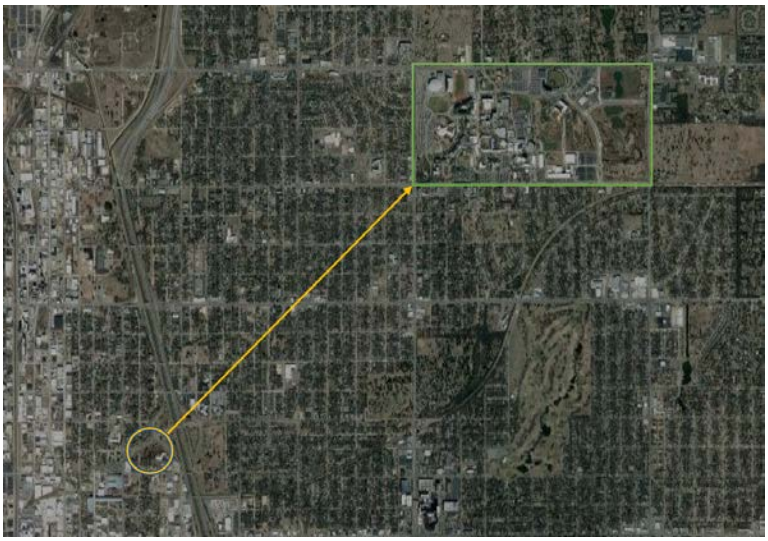

Figure 3.3: TV channel 15 transmitter location (yellow box) with respect to the university campus location (green box)

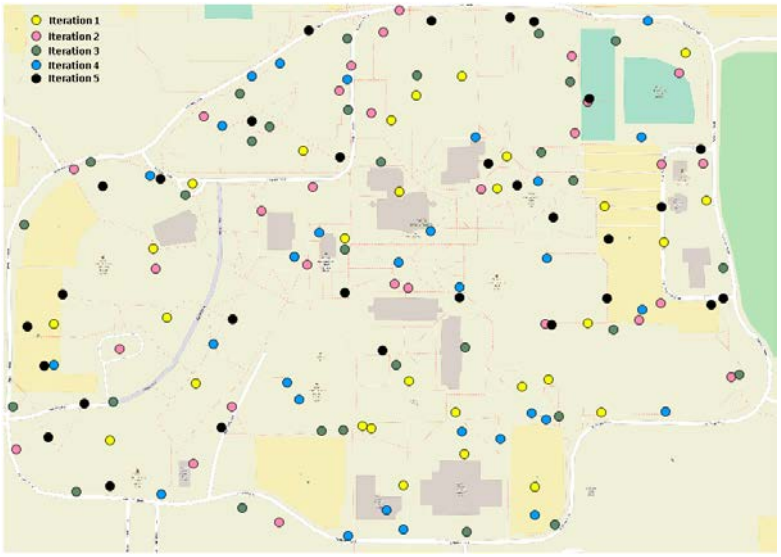

Figure 3.4: Additional measurement locations at each round

3.4.1 PSD prediction and error map construction

To create the PSD field heatmap, the campus area map is descretized into a grid. The PSD field heatmap is then created using the spatial predictions made for the locations in the grid. Our framework is run for the total number of five iterations so that the global predication error is smaller than 45. At the first iteration, the algorithm has 29 randomly selected sampling locations as the initial inputs. After each iteration, a set of 30 additional locations, along with their PSD measurement are injected into the framework. The PSD measurement locations have been demonstrated in Fig. 3.4 and the resulting PSD maps after first, third and fifth iteration, are demonstrated in Figs. 3.5. Fig. 3.5 (right) indicate that with the growing number of iterations, the prediction error at different locations is progressively reduced, which increases the reliability of the spatial predictions. Since the predication error in Eq. (3.10) is defined as the PSD field variance, the ”true” PSD value at each location is equal to the predicated PSD values (Fig. 3.5 (left)) plus the squared-root of the prediction error. The ”true” PSD value lower than -114 dBm, e.g., digital TVWS threshold, indicates the underutilized spectrum, known as white space at those locations. Moreover, the left plot in Figure 3.6 represents the decreasing level of global prediction

error with the increase in the number of iterations. This is essentially due to the growing number of observations at each iteration to provide predictions for non-sampling locations. Relying on the final spectrum map(Fig. 3.5 left sub-plot 3) and campus map (Fig. 3.3), abundant white spaces are observed in the middle areas of the campus. This is justified by signal degradation in the presence of barriers such as buildings and trees. There is no available TVWS in the west and southeast areas of the campus, which are the nearmost areas to the TV base station with no major signal degrading barriers. The northwest area of the campus is in the farmost distance from the TV base station and located behind all the buildings, which cause the existance of significant availability of white spaces. It is important that the presence of spectrum opportunities in different areas of the campus is in contradiction with information provided in conventional geolocation databases. For example, in Google spectrum database, TV channel 15 is inaccurately represented as unavailable in the entire town in which our university campus is located.

3.4.2 Comparison with conventional Kriging algorithm

An advantage of our proposed framework is its ability to provide a more accurate assessment of the prediction error compared with the conventional Kriging algorithm. The conventional Kriging algorithm underestimates the prediction error at different locations due to ignoring the inherent variability in the unknown parameters. To demonstrate the more accurate assessment of the prediction error provided by our proposed framework, we include the outputs of the Kriging algorithm in this demonstration as follows. At each iteration of the experiments, after selecting additional sampling locations, Kriging algorithm with augmented data is executed in addition to the Bayesian spatial prediction phase of our framework. Note that Kriging algorithm evaluates the conditional variance of the noisy measurement process based on the parameter estimates fitted through empirical variogram. However, our Bayesian decision framework assesses this value through marginalizing the computations over the posterior distribution of the parameters. On the right plot in Fig. 3.6, the prediction error value of the Kriging algorithm and our Bayesian

decision framework at each iteration is compared to the true variance of the measurement process provided by the unbiased estimation via the sample variance of all the PSD measurements (dotted line). It is evident that at each iteration, our Bayesian decision framework yields the more accurate representation of the prediction error provided compared to the Kriging algorithm.

3.5 Conclusion

In this paper, we have proposed an iterative Bayesian decision framework towards a cloud-based crowd-augmented spectrum mapping system for TVWS identifications. Our proposed methodology iteratively increases the accuracy of the PSD spatial predictions by selecting additional locations for spectrum sensing, to expectedly maximize the global prediction error reduction over multiple sampling rounds. The uncertainty of the parameters in the underlying spatial model has been addressed in an online manner by marginalizing the Bayesian spatial prediction and error calculations on the posterior distribution of the parameters estimated through MCMC simulations at each round. We have demonstrated that this approach promotes more accurate inference of the underlying model as well as the field spatial prediction compared to the conventional Kriging algorithm. The proposed scheme has been evaluated by studying our University main campus for TVWS discovery. Abundant spectrum opportunities have been observed in different areas of the campus despite the inaccurate information provided by conventional geolocation databases.

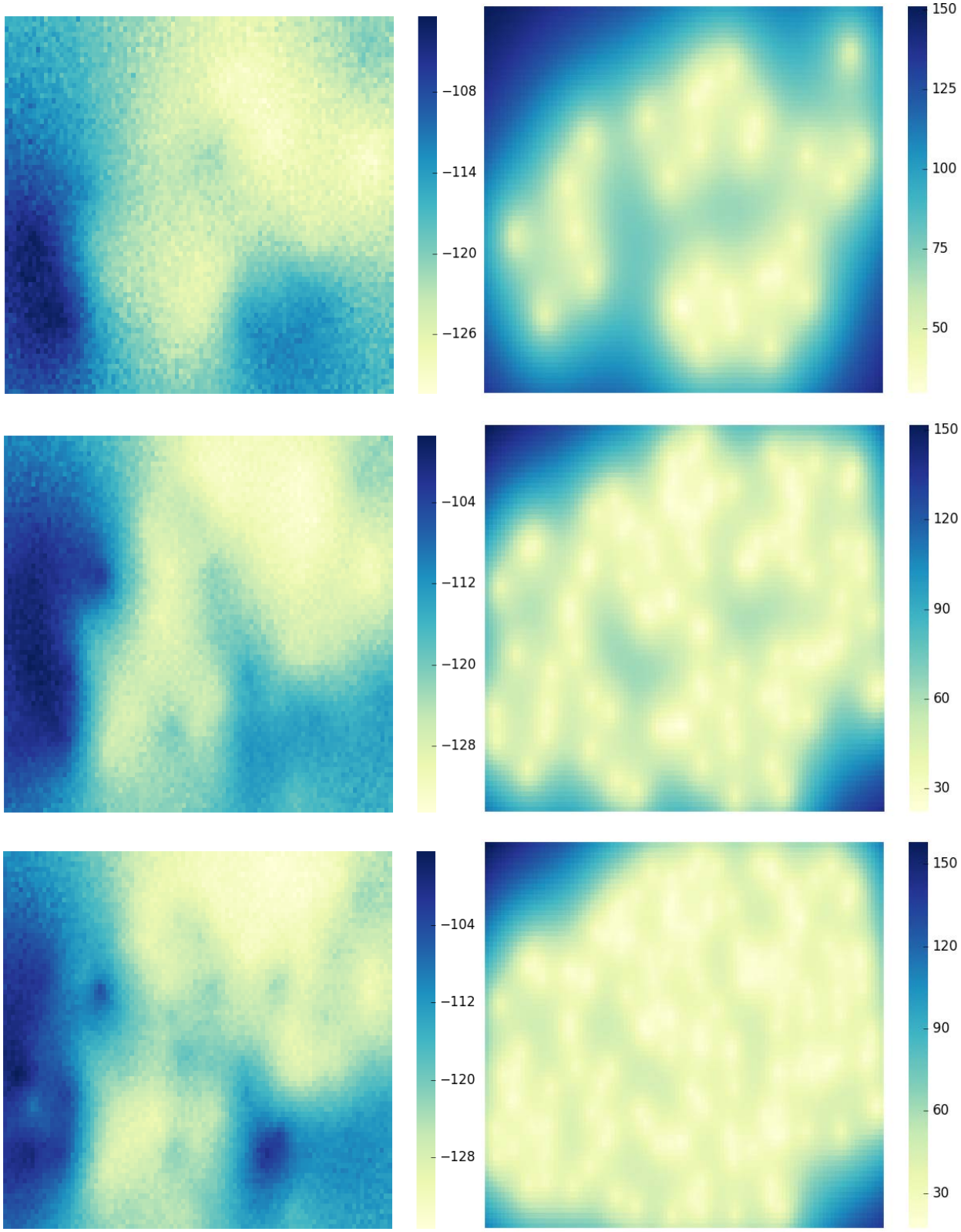

Figure 3.5: (left) PSD spatial prediction; (right) PSD prediction error (first, third and fifth iterations)

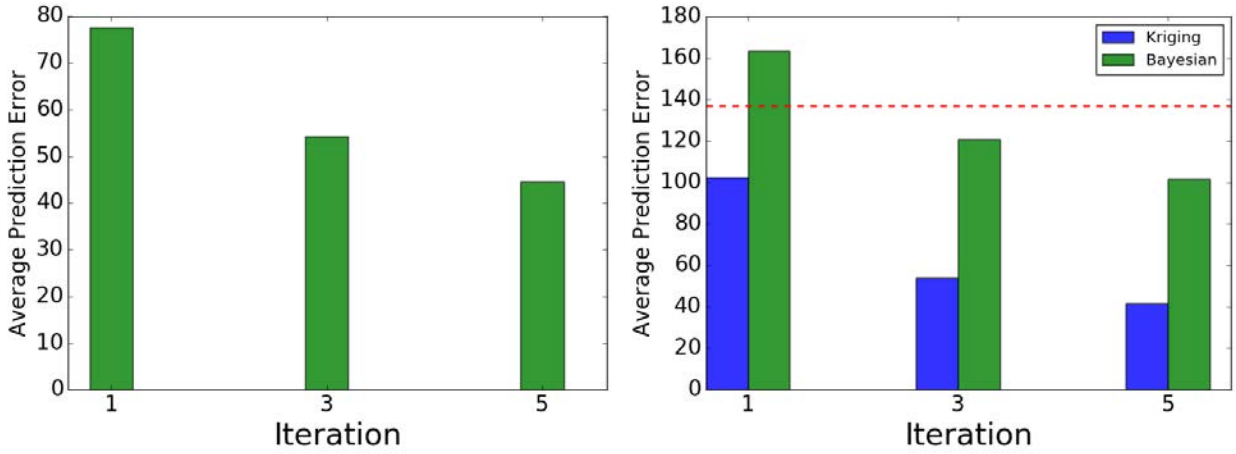

Figure 3.6: (left) Average prediction error of the signal process in Bayesian decision framework; (right) Average prediction error of the measurement process in Kriging algorithm versus Bayesian decision framework compared to the unbiased estimate of the measurement process variance (dotted line)

CHAPTER 4

COOPERATIVE KRIGED KALMAN FILTER FOR SCALAR RANDOM FIELD EXPLORATION WITH MOBILE SENSOR NETWORKS

4.1 Introduction

In this chapter, we propose a framework designed for dynamic random field exploration utilizing mobile sensor networks. A mobile sensor network comprises of a group of robotic agents each equipped with sensors, networking and computational units. The agents in the network can perform sensing, process the data locally and propagate the data and results to other agents in the network. Examples of this are underwater swarming robots (USR) which may consist of multiple autonomous underwater vehicles (AUVs) equipped with a hydophone to sense the signal in the form of sound pressure level. The sensed signal can then be processed and propagated over the network utilizing the computational and networking features.

Utilization of mobile sensor networks facilitates real-time random field exploration adaptive to the underlying dynamic nature of the field. Starting at an initial location, agents perform field sensing, cooperatively process the collected data utilizing the information obtained during exploration so far and then select the next sampling locations accordingly depending on the exploration objective. Although it seems highly appealing in terms of cost-effectiveness and envionmental adaptability, significant challenges are imposed, as pertaining to model and mapping accuracy considering that measurements become available over time. This implies the necessity of the presence of a methodology to well-utilize limited amount of measurements which are often noise-corrupted and adaptively include the growing information during exploration. Also, the high degree of interrelation between formation, trajectory and mapping tasks imposes additional challenges. In fact, the performance of a mapping scheme utilized in a mobile sensor network is highy depended on the sampling locations. This needs an intelligent mechanism during exploration to provide

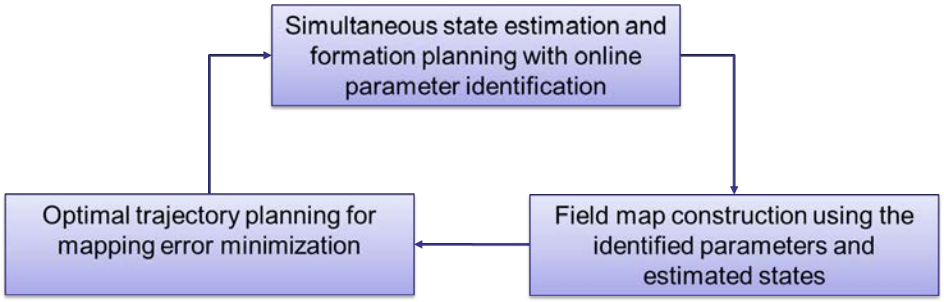

Figure 4.1: Joint sensing-motion-mapping co-design

the agents on recommended sampling locations in the form of formation and trajectory. In this case, design of a proper scheme which addresses all the mentioned challenges for real-time field map construction can be very complex.

In this paper, we address the problem of scalar random field exploration by mobile sensor networks, with the random field characterized by the Gaussian processes. We develop a joint sensing-motion-mapping scheme consisting of three major subtasks: (1) Online parameter identification, simultaneous state estimation and formation planning using a coopeartive Kalman filter (2) Field map construction utilizing the identified parameters and estimated state. (3) Optimized trajectory planning to navigate the agents along the information-rich paths.

The computations involved in the proposed scheme can be performed by a designated agent in the network. With a proper communication infrastructure, the measurements taken by all agents can be sent to the designated agent, where state estimation, formation planning, parameter identification and trajectory planning take place. The individual agents will then be provided with the updated formation/trjectory settings to obtain field measurements. Meanwhile, map reconstruction can be performed locally in the designated agent or in a cloud server provided with the required information from the designated agent. We particularly evaluate our proposed framework by simulating two different environments, i.e. an underwater acoustic channel with a time-varying impulse response

and the advection-diffusion process. Details about the simulations are provided in chapter 5.

4.2 Joint Sensing-Motion-Mapping Co-design

We consider a mobile sensor network with N robotic agents where the field measurement observed by each agent $i \in \{1, 2, ..., N\}$ is modeled as

$$y(r_{i,t}, t) = z(r_{i,t}, t) + \varepsilon(r_{i,t}, t) \tag{4.1}$$

where $r_{i,t} \in \mathbb{R}^2$ denotes the position of the agent i at time t. $z(r_{i,t}, t) \in \mathbb{R}$ denotes the value of the field at time instance t for $r_{i,t}$ and . $y(r_{i,t}, t) \in \mathbb{R}$ indicates the realization of $z(r_{i,t}, t)$ which is corrupted with the spatio-temporally white Gaussian noise, i.e. $\varepsilon(r_i, t) \sim \mathcal{N}(0, \sigma_\varepsilon^2)$. Following[12] and [54], the random field process, $z(r_{i,t}, t)$, can be modeled as:

$$z(r_{i,t}, t) = \mu(r_{i,t}, t) + \nu(r_{i,t}, t) \tag{4.2}$$

where mean $\mu(r_{i,t}, t)$ is the spatio-temporally correlated component of the field and the process noise $\nu(r_{i,t}, t) \sim \mathcal{N}(0, \sigma_\nu^2)$ is the Gaussian stationary random process which is spatially correlated but temporally white. At an arbitrary location x, $\mu(x, t)$, is assumed to be a spatio-temporal random variable which evolves as

$$\mu(x, t) = \int_{\mathcal{A}} w(x, u)\mu(u, t-1)du + \eta(x, t) \tag{4.3}$$

where $\eta(x, t) \sim \mathcal{N}(0, \sigma_\eta^2)$ ia a spatially correlated yet temporally white Gaussian stationary random processes. The spectral density representation of the Eq. (4.3) is known as the Kriged Kalman Filter (KKF) model, see [12], [34]. As proposed in [54], the infinite dimensionality of KKF model in Eq. (4.3) can be reduced using an infinite set of continiously differentiable orthonormal bases, $\{\phi_k(.)\}_{k=1}^{\infty}$, truncted with $K \in \mathbb{Z}^+$ dominant components:

$$\mu(x, t) = \sum_{k=1}^{K} \alpha_k(t)\phi_k(x) \tag{4.4}$$

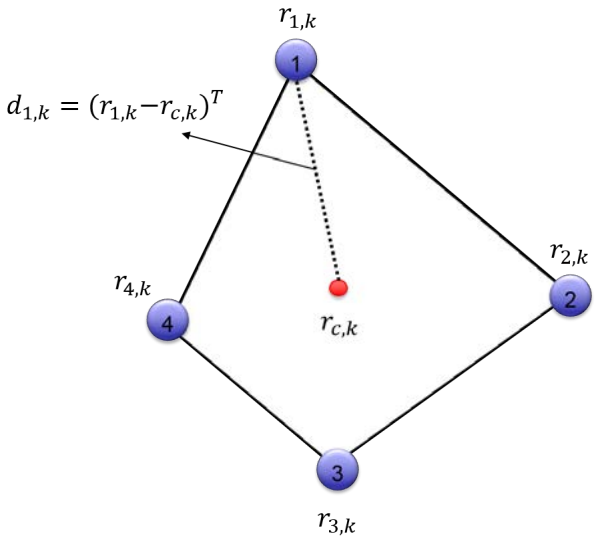

Figure 4.2: Formation of 4 agents in a mobile sensor network

$$w(x,u) = \sum_{k=1}^{K} \beta_k(x)\phi_k(u) \tag{4.5}$$

Using the above formulations, Eq. (4.3) can be represented as:

$$\phi^T(x)\alpha(t) = \beta^T(x)\alpha(t-1) + \eta(x,t) \tag{4.6}$$

where $\phi^T(.) \in \mathbb{R}^K$, $\alpha(.) \in \mathbb{R}^K$ and $\beta^T(.) \in \mathbb{R}^K$. This model has been widely studies in various contexts and extensions [11], [26], [28].

At each time step t, the function $\mu(r_{i,t}, t)$ can be approximated using Taylor series expansion around the centroid of the network, $r_{c,t}$, see also [60] and [58]. Assuming $\mathbf{x}_{i,t} = (r_{i,t}, t) \in \mathbb{R}^3$ and $\mathbf{x}_{c,t} = (r_{c,t}, t) \in \mathbb{R}^3$, the multivariate Taylor series expansion of $\mu(\mathbf{x}_{i,t})$ up to the first order can be stated as:

$$\mu(\mathbf{x}_{i,t}) \approx \mu(\mathbf{x}_{c,t}) + [(\mathbf{x}_{i,t} - \mathbf{x}_{c,t}).\nabla_{\mathbf{x}_{i,t}}\mu(\mathbf{x}_{c,t})] \tag{4.7}$$

where $\mu(\mathbf{x}_{c,t}) = \phi^T(r_{c,t})\alpha(t)$. This enables us to obtain the overall state-space model based on the network formation at each time step. The resulting model can then

be used for optimal formation planning based on the optimal estimation of the basis expansion coefficients, i.e. system state, in Eqs. (4.4) and (4.5). By modeling the field value at the network centroid using Eq. (4.3) and replace Eq. (4.3) into Eq. (4.7), we obtain the following:

$$\mu(\mathbf{x}_{i,t}) \approx \phi^T(r_{c,t})\alpha(t) + (r_{i,t} - r_{c,t})^T \nabla_{r_{i,t}} \phi^T(r_{c,t})\alpha(t) \tag{4.8}$$

Note that since the Taylor approximation of $\mu(\mathbf{x}_{i,t})$ is around $\mu(\mathbf{x}_{c,t})$, both at the same time step but different spatial locations, therefore the terms corresponding to the gradient with respect to the time component are eliminated from Eq. (4.7). Let $C \in \mathbb{R}^{N\times 3}$ and $\Psi \in \mathbb{R}^{3\times K}$ represent the following matrices:

$$C = \begin{bmatrix} 1 & (r_{1,t} - r_{c,t})^T \\ \vdots & \vdots \\ 1 & (r_{N,t} - r_{c,t})^T \end{bmatrix} \tag{4.9}$$

$$\Psi = \begin{bmatrix} \phi^T(r_{c,t}) \\ \nabla \phi^T_{r_{i,t}}(r_{c,t}) \end{bmatrix} \tag{4.10}$$

Then Eq. (4.8) can be reformulated by using Eq. (4.11) in order to represent the closed-form eqation with respect to all agents in the network.

$$M(t) \approx C\Psi\alpha(t) \tag{4.11}$$

Let $\phi(s) = [\phi_1(s), \phi_2(s), ..., \phi_k(s)]^T \in \mathbb{R}^{K\times 1}$ represent the basis functions evaluated at a location s, and let $\Phi = [\phi(r_{1,t}), \phi(r_{2,t}), ..., \phi_(r_{N,t})]^T \in \mathbb{R}^{N\times K}$ represent the basis functions evaluated at the agents coordinates. By evaluating the basis functions at agents coordinates, Ψ can be obtained as:

$$\Psi = C^\dagger \Phi \tag{4.12}$$

Where $C^\dagger$ is the pseudo-inverse of C. The closed-form of the overall state-space model with respect to all agents can be obtained by defining $B = [\beta(r_1), ..., \beta(r_N)] \in \mathbb{R}^{N\times K}$ and

$\eta(t) = [\eta(r_1, t), ..., \eta(r_N, t)] \in \mathbb{R}^{N \times K}$. By letting $A = C\Psi$ and substituting A into Eq. (4.6) we can obtain the state dynamics as follows:

$$A\alpha(t) = B\alpha(t-1) + \eta(t) \tag{4.13}$$

$$\alpha(t) = A^{\dagger}B\alpha(t-1) + A^{\dagger}\eta(t) \tag{4.14}$$

where $A^{\dagger}$ represents the pseudo-inverse of A. Therefore, defining $H = A^{\dagger}B$ as the state transition matrix, the overall state-space model is obtained as:

$$\begin{aligned} \mathbf{y}(t) &= A\alpha(t) + \nu(t) + \varepsilon(t) \\ \alpha(t) &= H\alpha(t-1) + A^{\dagger}\eta(t) \end{aligned} \tag{4.15}$$

4.2.1 Optimal Formation Planning

The state-space model (4.15) is in the standard linear form for which we can design a Kalman filter to sequentially find the distribution of the system state, $\alpha(t)$. With $Y_{0:t}$ defined as $\{Y(0) = \mathrm{y}(0), Y(1) = \mathrm{y}(1), ..., Y(t) = \mathrm{y}(t)\}$, $\hat{\alpha}(t|t) = \mathbb{E}[\alpha(t)|Y_{0:t}]$ and $\hat{\alpha}(t|t-1) = \mathbb{E}[\alpha(t)|Y_{0:t-1}]$, following the standard procedure [45], the cooperative Kalman filter can be expressed using the following equations for state estimation and one-step ahead prediction along with the corresponding error covariance matrices:

$$\hat{\alpha}(t|t) = \hat{\alpha}(t|t-1) + K(t)(\mathrm{y}(t) - A\hat{\alpha}(t|t-1)) \tag{4.16}$$

$$P(t|t) = (I - K(t)A)P(t|t-1)(I - K(t)A)^T + K(t)(C_\nu + C_\varepsilon)K(t)^T \tag{4.17}$$

$$\hat{\alpha}(t|t-1) = H\hat{\alpha}(t-1|t-1) \tag{4.18}$$

$$P(t|t-1) = HP(t-1|t-1)H^T + A^{\dagger}C_\eta A^{\dagger T} \tag{4.19}$$

$$K(t) = P(t|t-1)A^T(C_\nu + C_\varepsilon + AP(t|t-1)A^T)^{-1} \tag{4.20}$$

where $K(t) \in \mathbb{R}^{K \times N}$ indicates the Kalman gain at time step t. The error covariance matrix in Eq. (4.17) depends on the formation i.e. shape and size, of the network represented

by A. Therefore at each time step t, we can determine the network optimal formation by finding the optimal state estimation such that the sum of the mean squared errors, i.e. Eq. (4.21) is minimized:

$$J(t) = \mathrm{tr}[(I - K(t)A)P(t|t-1)(I - K(t)A)^T + K(t)(C_\nu + C_\varepsilon)K(t)^T] \tag{4.21}$$

This implies that at each time step, the optimal settings for the network formation is essentially updated using all the information obtained by the agents throughout the exploration. Additionally it is necessary to pose a constraint on the maximum size of the network for two reasons: (1) ensure robust communication between agents and the central agent depending on the communication range. (2) preserve the precision of the approximation for the spatio-temporal field given by the second order Taylor series expansion, Eq. (4.8). If agents in the network are far spread out, the Taylor expansion up to the first order is insufficient and higher orders are needed to properly approximate the field. Also, the minimum network size is also constrained since if the network is too dense, the spatial variation of the field will not be efficiently captured. With all the information discussed so far, the optimal formation planning problem can be states as follows:

$$\begin{aligned} &\min_{A} \quad J(t) \\ &\text{s.t.} \quad l_{min} \leq \|r_{i,t} - r_{c,t}\| \leq l_{max} \quad i \in \{1, ..., N\} \end{aligned} \tag{4.22}$$

where l_{min} represents the minimum distance between each agent and the central agent. Similarly l_{max} represents the maximum distance between each agent and the central agent. The optimization problem in (4.22) can be solved by numerical optimization techniques for optimal or near optimal formation.

4.2.2 Optimal Field Mapping

With the new observations becoming available at every time step, field map construction can be performed locally on the central agent or on a remote server with high computational power in the scenario of network availability. For this purpose, we use

the widely-adopted exponential functions to model the spatial correlation of the random processes $\nu(t)$ between two different spatial coordinates, Eq. (4.23). The exponential function is widely adopted to characterize the impact of fading [50] and [42].

$$C_\nu(x, x') = \sigma_\nu^2 \exp(-\delta_\nu \left\| x - x' \right\|^2) \tag{4.23}$$

The parameters of this exponential function can be obtained by the LS fitting method explained in [26], Appendix B. Let $\mathbf{x} = \{x_1, x_2, ..., x_m\}$ denote the set of locations at which the field is to be estimated. Let $\Sigma_{\mathrm{xx}} \in \mathbb{R}^{m \times m}$ represent the matrix with the element in row i and column j as $C_\nu(x_i, x_j)$. Also let $\Sigma_{\mathrm{xy}} \in \mathbb{R}^{N \times m}$ represent the matrix with the element in row i and column j as $C_\nu(r_{i,t}, x_j)$. Let $z(\mathbf{x}, t)|\mathrm{y}(t)$ denote the random variable representing the true field value with the knowledge of $\mathrm{y}(t)$. Then $\mathbb{E}[z(\mathbf{x}, t)|y(t)]$ is the optimal predictor of the true field as it is an unbiased estimator and has the minimum mean squared prediction error among all possible predictors.

$$\mathbb{E}[z(\mathbf{x}, t)|\mathrm{y}_{1:t}] = \Phi^T(\mathbf{x})\hat{\alpha}(t|t) + \Sigma_{\mathrm{xy}}^T(C_\nu + C_\varepsilon)^{-1}(\mathbf{y}(t) - A\alpha(\hat{t}|t)) \tag{4.24}$$

$$\begin{aligned} \mathrm{var}[z(\mathbf{x}, t)|\mathrm{y}_{1:t}] = \Sigma_{\mathrm{xx}} - \Sigma_{\mathrm{xy}}^T(C_\nu + C_\varepsilon)^{-1}\Sigma_{\mathrm{xy}} + \\ (\Phi^T(\mathbf{x}) - \Sigma_{\mathrm{xy}}^T(C_\nu + C_\varepsilon)^{-1}A)P(t|t)(\Phi^T(\mathbf{x}) - \Sigma_{\mathrm{xy}}^T(C_\nu + C_\varepsilon)^{-1}A)^T \end{aligned} \tag{4.25}$$

where Eqs. (4.24) and (4.25) indicate the Universal Kriging predictor mean and variance of the random field $[\mathbf{z}(s, t)|\mathrm{y}(\mathrm{t})]$ [11].

4.2.3 Optimal Trajectory Planning

The network trajectory planning scheme is coupled with the field exploration objective. Among the uses of mobile sensor networks for random field exploration, commonly pursued objectives are field mapping, source seeking, level curve tracking, source avoidance. Combined network trajectory planning schemes have also been presented [9]. Trajectories of the swarming robots greatly affect the accuracy of parameter identification and

mapping since the information content of the signals with respect to the distributed state varies from location to location. Therefore, the real-time information should be utilized to move the robots along the information-rich paths that can increase the performance of parameter identification and map construction.

For the purpose of field mapping, at each time step the neighbour locations at a particular neighborhood size around the current network centroid are considered as the candidate for the network centroid in the next time step. The mapping predictive variance at these candidate locations are decoupled from the field measurements as observed in Eq. (4.25). We take advantage of this property and design the error minimizing trajectory such that in the next location for the network centroid, the predictive variance in Eq. (4.25) is maximum compared to all other candidate locations. Therefore, the robots are navigated to the areas with larger uncertainties involved to provide more informative data in a greedy fashion.

Additionally, the network trajectory may be designed for source seeking where robots trace the maximum field intensity. In this case, at each time step t with the step size or learning rate of γ_t, the reference trajectory for the network for the next time step $r^*_{c,t+1}$, will be proposed based on the gradient ascent rule on the estimated field:

$$\nabla_s(\hat{z}(s,t)|\mathbf{y}_{1:t})\Big|_{s=r_{c,t}} = \nabla_s\phi^T(r_{c,t})\hat{\alpha}(t|t) + \nabla_s\Sigma^T_{r_{c,t},\mathrm{y}}(C_\nu + C_\varepsilon)^{-1}(\mathbf{y}(t) - A\hat{\alpha}(t|t)) \tag{4.26}$$

$$r^*_{c,t+1} = r_{c,t} + \gamma_t\nabla_s(\hat{z}(s,t)|\mathbf{y}_{1:t})\Big|_{s=r_{c,t}} \tag{4.27}$$

4.2.4 Online Parameter Identification

The state-space model mentioned in Eq. (4.15) is subject to uknown parameters, C_ϵ and C_ν, C_η and H. Therefore the optimal formation planning in Section 2.1, parameter identification in Section 2.2 and optimal trajectory planning in Section 2.3 need a proper estimate of these unknown parameters. In [53], [2], [43] and [24], fully Bayesian hierarchical methods have been proposed for the purpose of parameter identification,

where the likelihood function is multiplied by the prior density distribution of the unknown parameters to obtain the posterior parameter distribution. Then, based on the posterior distribution and the full conditional distribution of each unknown parameter, a Gibbs sampling procedure is followed to draw samples of the unknown parameters. Standard moment estimation of the unknown parameters have also been presented in [54] and [26]. Online parameter identification schemes based on sequential Monter Carlo (SMC) for general state-space models have also been described in [3] and [25]. However, since the model utilized in this research is a linear Gaussian state-space model and the closed-form derivation of the PDF for noise terms with respect to unknown parameters can be easily obtained analytically, the parameter estimation algorithm introduced in [44] can be customized for our application. This algorithm is based on the Maximum Likelihood (ML) technique within the iterations of the Expection Maximization (EM) scheme. The unknown parameters are estimated through a set of forward and backward iterations, i.e. Kalman filtering and smoothing, based on the distribution of the system state at the initial time step. We aim to utilize this methodology in an online strategy based on the slide-window concept as in [31]. Therefore, the estimates of the unknown parameters are updated at the end of each slide-window.

At the end of every slide-window of size w, the measurements $\mathrm{y}(t)$ and basis functions at agent coordinates $\Phi(t)$ are available for $t \in [n-w+1, n]$. We will use these information in order to update the estimate of the unknown parameters as follows. Let $R = C_\nu + C_\varepsilon$ represent the covariance matrix of the zero-mean random variable $\epsilon = \nu + \varepsilon$ and $Q = \Phi^\dagger C_\eta \Phi^{\dagger T}$ represent the covariance matrix of the zero-mean random variable $\zeta = \Phi^\dagger \eta$. The observation noise covariance matrix can be obtained as $C_\varepsilon = \sigma_\varepsilon^2 I$ where σ_ε^2 can be obtained during sensor calibration as mentioned in [26] and [54]. Therefore, if an estimate of R is available as a result of parameter identification, the estimate of background noise covariance matrix is obtained as $C_\nu = R - C_\varepsilon$. Therefore, let the hyper-parameter vector of the unknown parameters be represented as $\Theta = [R, Q, H]$. The joint

log-likelihood of the data given the model parameters $L(\Theta|\mathrm{y}_{n-w+1:n})$, within the window of size w until the current time step n, can then be represented as:

$$\begin{aligned}\ln(L) = -\frac{w}{2}\ln|R| - \frac{1}{2}\sum_{t=n-w+1}^{n}\epsilon(t)^T R^{-1}\epsilon(t) \\ -\frac{w}{2}\ln|Q| - \frac{1}{2}\sum_{t=n-w+1}^{n}\zeta(t)^T Q^{-1}\zeta(t) \\ -\frac{1}{2}\ln|\Sigma| - \frac{1}{2}(\alpha(n-w)-\mu)^T\Sigma^{-1}(\alpha(n-w)-\mu)\end{aligned} \tag{4.28}$$

$$\begin{aligned}\ln(L) = -\frac{w}{2}\ln|R| - \frac{1}{2}\sum_{t=n-w+1}^{n}(\mathrm{y}(t)-\Phi(t)\alpha(t))^T R^{-1}(\mathrm{y}(t)-\Phi(t)\alpha(t)) \\ -\frac{w}{2}\ln|Q| - \frac{1}{2}\sum_{t=n-w+1}^{n}(\alpha(t)-H\alpha(t-1))^T Q^{-1}(\alpha(t)-H\alpha(t-1)) \\ -\frac{1}{2}\ln|\Sigma| - \frac{1}{2}(\alpha(n-w)-\mu)^T\Sigma^{-1}(\alpha(n-w)-\mu)\end{aligned} \tag{4.29}$$

The log-likelihood in (4.29) depends on the system state α which is unobserved and hidden. Therefore, the maximization of the log-likelihood function is performed with respect to the expectation of the hidden system state given the noisy observations y using EM algorithm. At each iteration of the EM algorithm, the unknown parameters in Θ are obtained as follows:

$$H = BA^{-1} \tag{4.30}$$

$$Q = \frac{1}{w}(C - HB^T) \tag{4.31}$$

$$R = \frac{1}{w}\sum_{t=n-w+1}^{n}[(\mathrm{y}(t)-\Phi(t)\hat{\alpha}(t|n))(\mathrm{y}(t)-\Phi(t)\hat{\alpha}(t|n))^T + \Phi(t)P(t|n)\Phi(t)^T] \tag{4.32}$$

where A, B and C are obtained using the following formulas:

$$A = \sum_{t=w-n}^{n-1}(P(t|n) + \hat{\alpha}(t|n)\hat{\alpha}(t|n)^T) \tag{4.33}$$

$$B = \sum_{t=w-n+1}^{n}(P(t,t-1|n) + \hat{\alpha}(t|n)\hat{\alpha}(t-1|n)^T) \tag{4.34}$$

$$C = \sum_{t=w-n+1}^{n} (P(t|n) + \hat{\alpha}(t|n)\hat{\alpha}(t|n)^T) \tag{4.35}$$

The derivation of these formulations has been detailed in [44]. Therefore, our customized algorithm for real-time parameter identification using agents in the network by employing the slide-window concept as the one followed in [31], is summerized as follows:

1. Initialize μ and Σ as well as the unknown parameters R, Q and H with proper values.

2. Use the Kalman filter and Kalman smoother in Appendix section of [44], in order to evaluate $\hat{\alpha}(t|n)$, $P(t|n), P(t, t-1|n)$ for $t \in [n-w, n]$.

3. Update the maximum likelihood estimates of the unknown parameters in Θ based on the information obtained in step 2 using Eqs. (4.30) (4.31) (4.32) for the current slide-window and update μ and Σ based on $\hat{\alpha}(n-w|n)$ and $P(n-w|n)$ obtained in Kalman smoothing in step 2.

5. If the termination criterion is met, stop. Otherwise, return to step 2. Termination criterion can be set as the maximum number of iterations or the nominal changes in the estimated value of the unknown parameters across consequetive iterations.

Based on our expeience, the naive implementation of the above algorithm results in run time numerical instability even after a few iterations of satisfactory performance. Therefore, we aim to maximize the robustness of this algorithm by a different implementation based on the concept introduced in [18] for a more generic state-space model. In particular, instead of propagating the full covariance matrices $P(t|t-1)$, $P(t|t)$ and $P(t|n)$ in forward and backward iterations, i.e. Kalman filtering and smoothing, of the EM algorithm, the square root filtered representations of these covariance matrices, i.e. $P(t|t-1)^{1/2}$, $P(t|t)^{1/2}$ and $P(t|n)^{1/2}$, obtained using appropriate matrix QR factorization are propagated. In the mean time, the corresponding state estimations can be obtained for example by replacing $P(t|t-1) = P(t|t-1)^{1/2}P(t|t-1)^{T/2}$. (See details in Section 4.3 [18]). The robust implementation of the EM algorithm guarantees a symmetric and positive semi-definite matrix A obtained in Eq. (4.33) at each iteration of the algorithm and therefore an update of H can be easily obtained by using Eq. (4.30). However evaluation

of Q directly using Eq. (4.31) might lead to numerical instability caused by potential loss of positive semi-definiteness property due to the subtraction operation. This has been comprehensively discussed in [18]. Therefore we utilize the Cholesky factorization as follows in order to update Q at each iteration so that the matrix positive semi-definiteness property is preserved:

$$\begin{bmatrix} A & B^T \\ B & C \end{bmatrix} = \begin{bmatrix} 1 & 0 \\ L_{21} & 1 \end{bmatrix} \begin{bmatrix} U_{11} & U_{12} \\ 0 & U_{22} \end{bmatrix}$$

And therefore:

$$Q = U_{22}^T U_{22} \tag{4.36}$$

Furthermore, in addition to unknown parameters, basis functions as functions of spatial coordinates are selected in advance. Among the commonly used basis functions including empirical basis functions [54], exponential basis functions [30] [9] [29] and Fourier series [39], we use a set of bivariate Legendre polynomials. A bivariate Legendre polynomial for a particular spatial coordinate on a plane can be constructed as the product of the univariate polynomials at each dimension. The univeriate legendre polynomial of order $l \in Z^+$ for $x \in [-1, 1]$ is represented by the following Rodrigues formula:

$$P_l(x) = \frac{1}{2^l \; l!} \; \frac{d^l}{dx^l}(x^2 - 1)^l \tag{4.37}$$

CHAPTER 5

APPLICATIONS OF COOPERATIVE KRIGED KALMAN FILTER WITH SIMULATIONS

Our introduced framework in Chapter 4 can be conveniently customized for different random field exploration objectives such as mapping, source seeking, level curve tracking, etc. depending on the agents navigation strategy. In this chapter, we utilize this framework for two different mapping applications using computer simulations. First, the underwater acoustic communication channel is simulated under a time-varying impulse response. Parameter mapping in a simulated underwater environment with linear time-invariant impulse response has been addressed in [55]. The identification of the underwater channel properties and their spatial-temporal variation is particularly of interest for efficient and effective underwater wireless networking. Second, we simulate the advection-diffusion field which has been conventionally adopted to characterize many physical processes in nature such as atmospheric and waterborne pollution transport [58].

In order to use our framework for the two simulated random fields, we simulate the environment by considering a square shaped area discretized into a grid. In the beginning, the agents are placed randomly on the grid with a particular network size. The random fields are simulated and used as inputs to our framework. After processing the measurements for parameter identification, formation planning and trajectory planning, the location of the agents are updated and new field measurements are generated through simulations. This procedure is repeated for a particular simulation run time.

5.1 Underwater Acoustic Communication Channel

The underwater acoustic communication channel in a shallow water is subject to signficant multipath effects caused by surface and bottom signal reflections. Figure (5.1) illustrates a simplified representation of the multipath environment in a shallow water where a signal from the transmitter reaches the receiver in multiple paths.

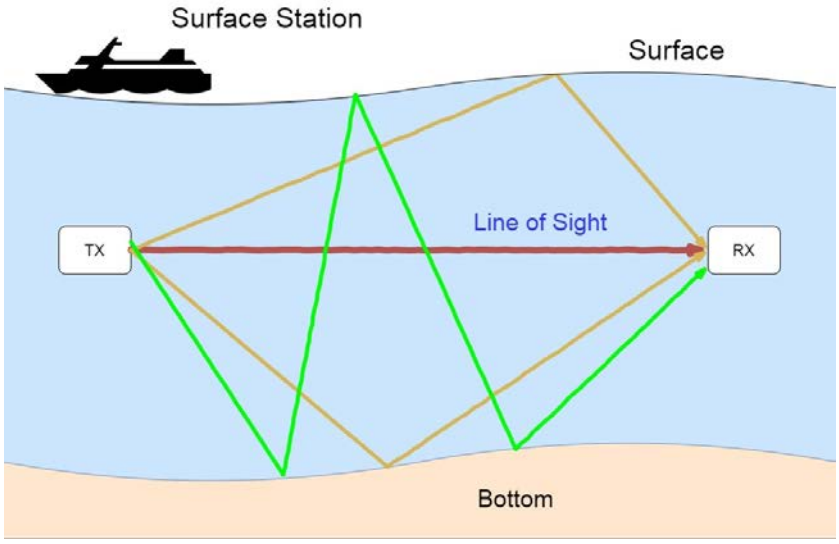

Figure 5.1: Underwater Acoustic Communication Channel under Multipath Effects

The time-varying impulse response of the underwater acoustic channel within a block of duration $T \in \mathbb{R}^+$, has been conventionally represented as [62], ch. 1:

$$h(t;\tau) = \sum_{p=1}^{N_{pa}} A_p(t)\delta(\tau - \tau_p(t)) \tag{5.1}$$

where $t \in [0, T]$ and T is in the scale of subseconds. N_{pa} denotes the number of paths along which the acoustic signals are propagated. $A_p(t)$ and $\tau_p(t)$ denote the amplitude and delay for the path p. Within each block, the amplitude is often considered as constant and the time-varying delay is represented by the first-order polynomial as $\tau_p(t) = \tau_p - a_p t$ where a_p represents the Doppler scaling factor for the path p. Therefore, the resulting channel impulse response, characterized by N_{pa} triplets $\{A_p, \tau_p, a_p\}$, is obtained as:

$$h(t;\tau) = \sum_{p=1}^{N_{pa}} A_p\delta(\tau - [\tau_p - a_p t]) \tag{5.2}$$

The Fourier transform of the channel impulse response in Eq. (5.2) gives the channel frequency response as:

$$H(t;f) = \int_{-\infty}^{\infty} h(t;\tau)e^{-j2\pi f\tau}d\tau = \sum_{p=1}^{N_{pa}} A_p e^{-j2\pi f(\tau_p - a_p t)} \tag{5.3}$$

For a system of the frequency range $[f_0 f_0 + B]$ where B indicates the bandwidth, the instantaneous channel gain can be defined as [41]

$$G(t) = \frac{1}{B} \int_{f_0}^{f_0+B} |H(t; f)|^2 df \tag{5.4}$$

We consider the instantaneous channel gain in Eq. (5.4) as the spatio-temporal field to be estimated where the spatial variation occurs due to the displacement of the receivers.

5.1.1 Channel simulation

Underwater environment and swarm control : The introduced swarming robots framework in Chapter 4 is applied to perform the underwater acoustic channel modeling. A shallow water environment is simulated consisting of 4 AUVs as receivers and 1 transmitter. Figure (5.2) illustrates an example of the underwater swarming robots (USR) communicating information with a surface station. The water surface is assumed to be varying in height with a flat surface. Both the transmitter and receivers are assumed to be located at 50 m depth. The channel modeling is performed along the horizontal plane between the receivers and the transmitter.

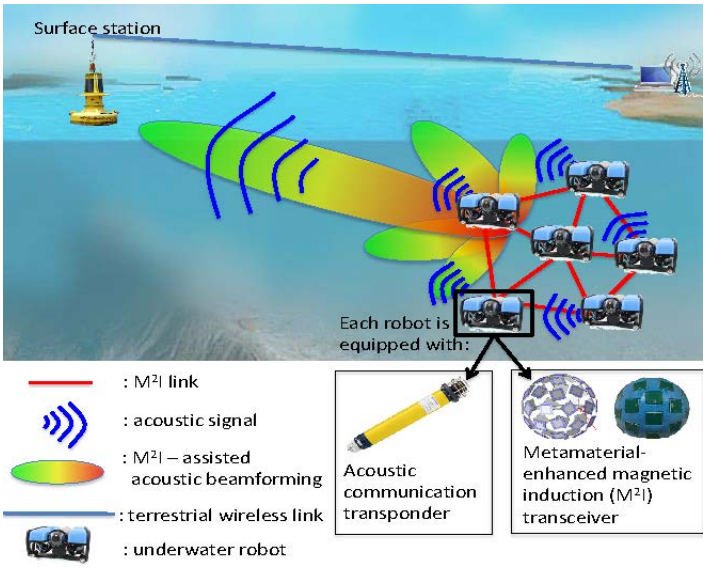

Figure 5.2: Underwater Swarming Robots

Acoustic channel modeling with multipath fading : In order to simulate the time-varying channel impulse response, we utilize the acoustic channel simulator introduced in [41]. However we ignore the effects of small-scale channel variations caused by signal scattering to avoid the model complexity. The Doppler effect is simulated considering transmitter and recievers drifting, receivers vehicular motion and surface motion. We assume that the transmitter is stationary and the Doppler effect created by the transmitter is only caused by its unintentional movement. We set this simulator to use BELLHOP software which mimics the multipath arrival of the acoustic waves based on ray tracing. In addition, we simulate the additive white Gaussian noise (AWGN) using the model introduced in [48]. The frequency dependant noise stems from 4 different sources including turbulence noise, shipping noise, surface motion noise and thermal noise.

5.1.2 Channel identification

Channel identification is performed by utilizing probing signals. The source transmits linear frequency modulated (LFM) signals at the pressure level of 185 dB, starting at the frequency of 12 kHz and linearly increasing to up 18 kHz over the course of 500 ms. The convolution of the transmitted signal with the channel impulse respose combined with the environmental noise gives the received signal as [23]:

$$
\begin{aligned}
y(t) = h(t;\tau) \circledast s(t) + w(t) = \\
&\int h(t;\tau)s(t-\tau)d\tau + w(t) = \\
&\sum_{p=1}^{N_{pa}} A_p \int \delta(\tau - (\bar{\tau_p} - \bar{a_p}t))s(t-\tau)d\tau + w(t) = \\
&\sum_{p=1}^{N_{pa}} A_p s(t - (\bar{\tau_p} - \bar{a_p}t)) + w(t) = \\
&\sum_{p=1}^{N_{pa}} A_p s((1+\bar{a_p})t - \bar{\tau_p}) + w(t)
\end{aligned}
\tag{5.5}
$$

where $\bar{\tau}_p$ and $\bar{a}_p$ represent the delay and Doppler scaling factor for the path p. Upon observing the received signal and since the transmitted probing signal is known, channel parameters can be identified at a receiver. Various methodologies have been presented in the past for this purpose including Matched Filtering, Matching Pursuit(MP) and Basis Pursuit Denoising (BPDN). We aim to use BPDN as it has demonstrated a superior performance compared with other methods [23]. We refer the interested readers to learn about BPDN in [23], but provide a very brief description of the procedure in the following. In order to perform channel identification, the Doppler scaling factor and delay related to each path are transformed as $\tau_p = \bar{\tau}_p/(1 + \bar{d}_p)$ and $d_p = 1 + \bar{d}_p$ so that Eq. (5.5) is represented in the matrix form as:

$$y = Sh + w \tag{5.6}$$

Then two sets of candidate values, also called dictionaries, are considered for path specific delay and Doppler scaling factor as

$$S_a = \{a_{\text{min}}, a_{\text{min}} + \Delta a, ..., a_{\text{max}}\} \tag{5.7}$$

$$S_\tau = \{0, \Delta\tau, 2\Delta\tau, ..., \tau_{\text{max}}\} \tag{5.8}$$

For each candidate value $a_i \in S_a$, a Toeplitz matrix, S_i is constructed with candidate values in S_τ as follows:

$$S_i = \begin{bmatrix} s(a_i 0) & 0 & \dots & 0 \\ s(a_i \Delta\tau) & s(a_i 0) & \dots & \vdots \\ \vdots & \vdots & \ddots & \vdots \\ s(a_i(N-1)\Delta\tau) & s(a_i(N-2)\Delta\tau) & \dots & s(a_i(N-N_\tau)\Delta\tau) \end{bmatrix}$$

Matrix S is then constructed as the concatenation of all the constructed Toeplitz matrices, i.e. $S = [S_1, S_2, ..., S_{N_d}]$. The problem of multipath channel identification is therefore rep-

resented as the following second order cone programming (SOCP) optimization problem:

$$\begin{aligned} &\min_{h} \|h\|_1 \\ &\text{s.t. } \|y - Sh\|_2 \leq \varepsilon \end{aligned} \tag{5.9}$$

where ε is set as the noise variance. Each non-zero element in the estimated h represents a path where the associated delay and Doppler scale factor can be identified with the index and the path amplitude is the value of the non-zero element. The identified paths are then used to reconstruct the channel frequency response over the bandwidth of the probing signal and channel gain is estimated as in Eq. (5.4). The estimated channel gain is then considered as the noisy field measurement input to the framework in chapter 4. In our future work, we are going to illustrate the simulation results for channel gain mapping under the mentioned settings.

5.2 Advection-Diffusion Processes

Many physical processes in particular atmospheric and waterborne pollution have been conventionally respresented by the advection-diffusion field which in 2D domain can be characterized by the following partial differential equation (PDE) [16] and [33]:

$$\frac{\partial z(r,t)}{\partial t} = D\nabla^2 z(r,t) + \nu^T \nabla z(r,t) \quad r \in \mathbb{R}^2 \tag{5.10}$$

where $z(r,t) \in \mathbb{R}$ is the field concentration at location r and time t, $D \in \mathbb{R}^+$ represents the diffusion coefficient, $\nu \in \mathbb{R}^2$ represents the flow velocity vector, ∇ is the gradient operator and ∇^2 is the Laplacian operator. The observations made by an agent in a swarm of robots are field values corrupted with white noise, represented as:

$$y(r,t) = z(r,t) + \varepsilon(r,t) \tag{5.11}$$

We simulate the advection-diffusion field with the finite difference method. The field measurement is then obtained as the field value combined with a random white noise, which is then fed as the noisy field measurement input to the framework in chapter 4.

Our initial results represent the satisfactory performance of the application of our framework for mapping of the advection-diffusion field. Figures (5.3) show the comparison of the true and estimated field values based on two different implementations. The left-hand side figure shows the comparison of the true and estimated field with the implementation that Q gets updated directly using Eq. (4.31). However, as explained in chapter 4, this approach is prone to numerical instabiliy and is not guaranteed to always give satisfactory results. On the other hand, the right-hand side figure demonstrates the results where Q is updated based on Cholesky factorization in Eq. (4.36) but under the same algorithmic settings as the left-hand side figure. This approach is numerically robust, however the undesired performance at some iterations is observed as convergence has not been reached in the EM algorithm for model parameter identification in the previous slide-window. This necessitates a careful selection of the convergence criterion to obtain satisfactory performance at consequetive iterations. Moreover, these figures show the mapping performance at the network centroid. In our future work, we will move on with investigating the performance for the locations that are distant from agents over the simulation time.

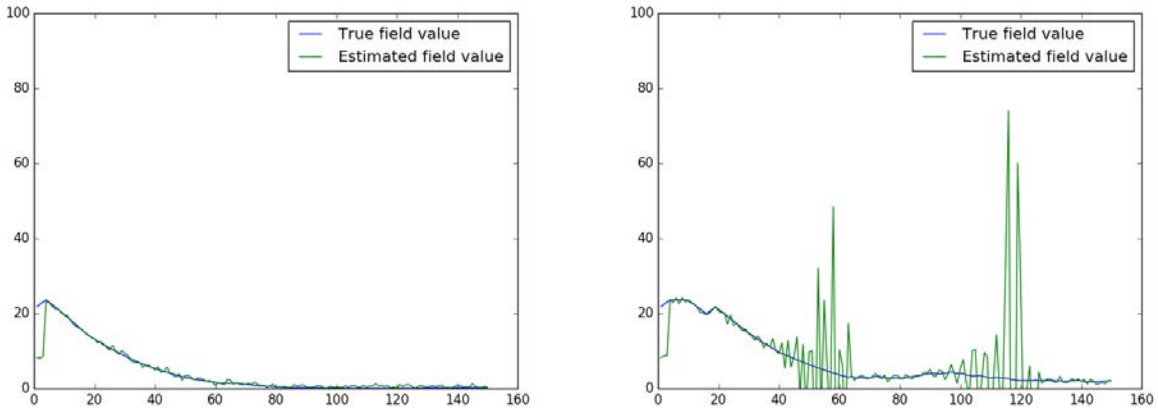

Figure 5.3: True and estimated field at the at the network centroid; (left) Q updated directly based on Eq. 4.31 (right) Q updated based on Cholesky factorization in Eq. 4.36

CHAPTER 6

CONCLUSIONS AND FUTURE WORKS

In this dissertation we have proposed two frameworks for large-scale online environmental mapping of scalar random fields in static and dynamic environments.

First, an iterative Bayesian decision framework has been developed for static spatial modeling. This framework is a combination of Bayesian spatial prediction and Bayesian experimental design with the objective of field map construction and incrementally increasing the accuracy through selecting additional locations for further sampling. This framework is applicable in the scenarios where the sensing devices are properly equipped to communicate with a cloud server as the centralized processing unit. This framework has been particularly applied for TVWS detection within the area of Wichita State University main campus. Remarkable spectrum opportunities were oserved in different areas of the campus.

Second, a cooperative field exploration scheme has been proposed, designed for mobile sensor network platforms, for dynamic spatial-temporal modeling. The proposed scheme addresses the field exploration by simultaneously addressing system state estimation and formation planning based on the growing information of the unknown field. The agents are then navigated along the information-rich paths for effective sampling. Parameter identification is performed at the end of each slide-window based on the data obtained within the window size. The performance of this framework is to be evaluated based on two different random field simulations. First an underwater acoustic channel is simulated with a time-varying channel impulse response, where the channel gain is considered as the random field to be reconstructed. Second, the advection-diffusion process is simulated, which is well-established for modelling the atmospheric and waterborne pollution.

In the future work we are going to illustrate the comprehensive computational re-

sults for the underwater acoustic communication channel and the advection diffusion process simulations. Furthermore, this research can be well-extended to cover more complicated challenges in the area of random field exploration. In particular, indoor environmental modeling is a possible extension which will be very interesting posing additional channel modeling complications due to the significant multipath effects. Also, 3-dimensional environments with obstacles can be considered for exploration with mobile sensor networks, which requires proper motion planning algorithms for effective navigation of robots. Tracing a static/moving target is another possible extension to our proposed framework.

REFERENCES

REFERENCES

[1] Piyush Agrawal and Neal Patwari. Correlated link shadow fading in multi-hop wireless networks. *IEEE Transactions on Wireless Communications*, 8(8), 2009.

[2] Fahimah A Al-Awadhi and Ali Alhajraf. Prediction of non-methane hydrocarbons in kuwait using regression and bayesian kriged kalman model. *Environmental and ecological statistics*, 19(3):393–412, 2012.

[3] Christophe Andrieu, Arnaud Doucet, and Vladislav B Tadic. On-line parameter estimation in general state-space models. In *Decision and Control, 2005 and 2005 European Control Conference. CDC-ECC'05. 44th IEEE Conference on*, pages 332–337. IEEE, 2005.

[4] Nikolay A Atanasov, Jerome Le Ny, and George J Pappas. Distributed algorithms for stochastic source seeking with mobile robot networks. *Journal of Dynamic Systems, Measurement, and Control*, 137(3):031004, 2015.

[5] Thomas Back. *Evolutionary algorithms in theory and practice: evolution strategies, evolutionary programming, genetic algorithms*. Oxford university press, 1996.

[6] Daniel Catrein and Rudolf Mathar. Gaussian random fields as a model for spatially correlated log-normal fading. In *Telecommunication Networks and Applications Conference, 2008. ATNAC 2008. Australasian*, pages 153–157. IEEE, 2008.

[7] Ayon Chakraborty and Samir R Das. Measurement-augmented spectrum databases for white space spectrum. In *Proceedings of the 10th ACM International on Conference on emerging Networking Experiments and Technologies*, pages 67–74. ACM, 2014.

[8] Kathryn Chaloner and Isabella Verdinelli. Bayesian experimental design: A review. *Statistical Science*, pages 273–304, 1995.

[9] Jongeun Choi, Joonho Lee, and Songhwai Oh. Biologically-inspired navigation strategies for swarm intelligence using spatial gaussian processes. *IFAC Proceedings Volumes*, 41(2):593–598, 2008.

[10] Jongeun Choi, Songhwai Oh, and Roberto Horowitz. Cooperatively learning mobile agents for gradient climbing. In *Decision and Control, 2007 46th IEEE Conference on*, pages 3139–3144. IEEE, 2007.

[11] Jorge Cortés. Distributed kriged kalman filter for spatial estimation. *IEEE Transactions on Automatic Control*, 54(12):2816–2827, 2009.

[12] Noel Cressie and Christopher K Wikle. Space-time kalman filter. *Encyclopedia of environmetrics*, 2002.

REFERENCES (continued)

[13] Peter Diggle and Søren Lophaven. Bayesian geostatistical design. *Scandinavian Journal of Statistics*, 33(1):53–64, 2006.

[14] Peter J Diggle, JA Tawn, and RA Moyeed. Model-based geostatistics. *Journal of the Royal Statistical Society: Series C (Applied Statistics)*, 47(3):299–350, 1998.

[15] PJ Diggle, PJ Ribeiro, and Model-based Geostatistics. *Springer Series in Statistics*. Springer, 2007.

[16] Bruce A Egan and James R Mahoney. Numerical modeling of advection and diffusion of urban area source pollutants. *Journal of Applied Meteorology*, 11(2):312–322, 1972.

[17] Charles J Geyer. Practical markov chain monte carlo. *Statistical science*, pages 473–483, 1992.

[18] Stuart Gibson and Brett Ninness. Robust maximum-likelihood estimation of multivariable dynamic systems. *Automatica*, 41(10):1667–1682, 2005.

[19] Walter R Gilks, Sylvia Richardson, and David Spiegelhalter. *Markov chain Monte Carlo in practice*. CRC press, 1995.

[20] Rishi Graham and Jorge Cortés. Spatial statistics and distributed estimation by robotic sensor networks. In *American Control Conference (ACC), 2010*, pages 2422–2427. IEEE, 2010.

[21] Carlos Guestrin, Andreas Krause, and Ajit Paul Singh. Near-optimal sensor placements in gaussian processes. In *Proceedings of the 22nd international conference on Machine learning*, pages 265–272. ACM, 2005.

[22] Prabhu Janakaraj, Pu Wang, and Zheng Chen. Towards cloud-based crowd-augmented spectrum mapping for dynamic spectrum access. In *Computer Communication and Networks (ICCCN), 2016 25th International Conference on*, pages 1–7. IEEE, 2016.

[23] Xue Jiang, Wen-Jun Zeng, and Xi-Lin Li. Time delay and doppler estimation for wideband acoustic signals in multipath environments. *The Journal of the Acoustical Society of America*, 130(2):850–857, 2011.

[24] Giovanna Jona Lasinio, Sujit K Sahu, and Kant V Mardia. Modeling rainfall data using a bayesian kriged-kalman model. 2007.

REFERENCES (continued)

[25] Nicholas Kantas, Arnaud Doucet, Sumeetpal Sindhu Singh, and Jan Marian Maciejowski. An overview of sequential monte carlo methods for parameter estimation in general state-space models. *IFAC Proceedings Volumes*, 42(10):774–785, 2009.

[26] Seung-Jun Kim, Emiliano Dall'Anese, and Georgios B Giannakis. Cooperative spectrum sensing for cognitive radios using kriged kalman filtering. *IEEE Journal of Selected Topics in Signal Processing*, 5(1):24–36, 2011.

[27] Ruofan Kong, Wenlin Zhang, and Yi Guo. Distributed estimation and tracking for radio environment mapping. In *American Control Conference (ACC), 2014*, pages 464–470. IEEE, 2014.

[28] Hung M La, Weihua Sheng, and Jiming Chen. Cooperative and active sensing in mobile sensor networks for scalar field mapping. *IEEE Transactions on Systems, Man, and Cybernetics: Systems*, 45(1):1–12, 2015.

[29] Hung Manh La and Weihua Sheng. Distributed sensor fusion for scalar field mapping using mobile sensor networks. *IEEE Transactions on cybernetics*, 43(2):766–778, 2013.

[30] Xiaodong Lan and Mac Schwager. A variational approach to trajectory planning for persistent monitoring of spatiotemporal fields. In *American Control Conference (ACC), 2014*, pages 5627–5632. IEEE, 2014.

[31] Ming Lei, Chongzhao Han, and Panzhi Liu. Expectation maximization (em) algorithm-based nonlinear target tracking with adaptive state transition matrix and noise covariance. In *Information Fusion, 2007 10th International Conference on*, pages 1–7. IEEE, 2007.

[32] Zhiyun Lin, Mireille Broucke, and Bruce Francis. Local control strategies for groups of mobile autonomous agents. *IEEE Transactions on automatic control*, 49(4):622–629, 2004.

[33] Daniel P Loucks, Eelco Van Beek, Jery R Stedinger, Jozef PM Dijkman, and Monique T Villars. *Water resources systems planning and management: an introduction to methods, models and applications*. Paris: Unesco, 2005.

[34] Kanti V Mardia, Colin Goodall, Edwin J Redfern, and Francisco J Alonso. The kriged kalman filter. *Test*, 7(2):217–282, 1998.

[35] Melanie Mitchell. *An introduction to genetic algorithms*. MIT press, 1998.

REFERENCES (continued)

[36] Maziar Nekovee, Tim Irnich, and Jorgen Karlsson. Worldwide trends in regulation of secondary access to white spaces using cognitive radio. *IEEE Wireless Communications*, 19(4), 2012.

[37] Chiu Y Ngo and Victor OK Li. Fixed channel assignment in cellular radio networks using a modified genetic algorithm. *IEEE Transactions on Vehicular Technology*, 47(1):163–172, 1998.

[38] Petter Ogren, Edward Fiorelli, and Naomi Ehrich Leonard. Cooperative control of mobile sensor networks: Adaptive gradient climbing in a distributed environment. *IEEE Transactions on Automatic control*, 49(8):1292–1302, 2004.

[39] Connie NKK Phan. *Kriged Kalman filtering for predicting the wildfire temperature evolution*. PhD thesis, University of Toronto (Canada), 2014.

[40] Caleb Phillips, Michael Ton, Douglas Sicker, and Dirk Grunwald. Practical radio environment mapping with geostatistics. In *Dynamic Spectrum Access Networks (DYSPAN), 2012 IEEE International Symposium on*, pages 422–433. IEEE, 2012.

[41] Parastoo Qarabaqi and Milica Stojanovic. Statistical characterization and computationally efficient modeling of a class of underwater acoustic communication channels. *IEEE Journal of Oceanic Engineering*, 38(4):701–717, 2013.

[42] Janne Riihijarvi, Petri Mahonen, Matthias Wellens, and Martin Gordziel. Characterization and modelling of spectrum for dynamic spectrum access with spatial statistics and random fields. In *Personal, Indoor and Mobile Radio Communications, 2008. PIMRC 2008. IEEE 19th International Symposium on*, pages 1–6. IEEE, 2008.

[43] Sujit K Sahu and Kanti V Mardia. A bayesian kriged kalman model for short-term forecasting of air pollution levels. *Journal of the Royal Statistical Society: Series C (Applied Statistics)*, 54(1):223–244, 2005.

[44] Robert H Shumway and David S Stoffer. An approach to time series smoothing and forecasting using the em algorithm. *Journal of time series analysis*, 3(4):253–264, 1982.

[45] Dan Simon. *Optimal state estimation: Kalman, H infinity, and nonlinear approaches*. John Wiley & Sons, 2006.

[46] Amarjeet Singh, Fabio Ramos, Hugh Durrant Whyte, and William J Kaiser. Modeling and decision making in spatio-temporal processes for environmental surveillance. In *Robotics and Automation (ICRA), 2010 IEEE International Conference on*, pages 5490–5497. IEEE, 2010.

REFERENCES (continued)

[47] Adrian FM Smith and Gareth O Roberts. Bayesian computation via the gibbs sampler and related markov chain monte carlo methods. *Journal of the Royal Statistical Society. Series B (Methodological)*, pages 3–23, 1993.

[48] Milica Stojanovic. On the relationship between capacity and distance in an underwater acoustic communication channel. *ACM SIGMOBILE Mobile Computing and Communications Review*, 11(4):34–43, 2007.

[49] Zhi Sun and Ian F Akyildiz. Spatio-temporal correlation-based density optimization in wireless underground sensor networks. In *Global Telecommunications Conference (GLOBECOM 2011), 2011 IEEE*, pages 1–5. IEEE, 2011.

[50] Sebastian S Szyszkowicz, Halim Yanikomeroglu, and John S Thompson. On the feasibility of wireless shadowing correlation models. *IEEE Transactions on Vehicular Technology*, 59(9):4222–4236, 2010.

[51] Mehmet C Vuran and Ian F Akyildiz. Spatial correlation-based collaborative medium access control in wireless sensor networks. *IEEE/ACM Transactions On Networking*, 14(2):316–329, 2006.

[52] Matthias Wellens, J Riihijarvi, Martin Gordziel, and P Mahonen. Spatial statistics of spectrum usage: From measurements to spectrum models. In *Communications, 2009. ICC'09. IEEE International Conference on*, pages 1–6. IEEE, 2009.

[53] Christopher K Wikle, L Mark Berliner, and Noel Cressie. Hierarchical bayesian space-time models. *Environmental and Ecological Statistics*, 5(2):117–154, 1998.

[54] Christopher K Wikle and Noel Cressie. A dimension-reduced approach to space-time kalman filtering. *Biometrika*, 86(4):815–829, 1999.

[55] Wencen Wu, Aijun Song, Paul Varnell, and Fumin Zhang. Cooperatively mapping of the underwater acoustic channel by robot swarms. In *Proceedings of the International Conference on Underwater Networks & Systems*, page 20. ACM, 2014.

[56] Xuhang Ying, Chang Wook Kim, and Sumit Roy. Revisiting tv coverage estimation with measurement-based statistical interpolation. In *Communication Systems and Networks (COMSNETS), 2015 7th International Conference on*, pages 1–8. IEEE, 2015.

[57] Xuhang Ying, Jincheng Zhang, Lichao Yan, Guanglin Zhang, Minghua Chen, and Ranveer Chandra. Exploring indoor white spaces in metropolises. In *Proceedings of the 19th annual international conference on Mobile computing & networking*, pages 255–266. ACM, 2013.

REFERENCES (continued)

[58] Jie You, Yufei Zhang, Mingchen Li, Kun Su, Fumin Zhang, and Wencen Wu. Cooperative parameter identification of advection-diffusion processes using a mobile sensor network. In *American Control Conference (ACC), 2017*, pages 3230–3236. IEEE, 2017.

[59] Fumin Zhang, Edward Fiorelli, and Naomi Ehrich Leonard. Exploring scalar fields using multiple sensor platforms: Tracking level curves. In *Decision and Control, 2007 46th IEEE Conference on*, pages 3579–3584. IEEE, 2007.

[60] Fumin Zhang and Naomi Ehrich Leonard. Cooperative filters and control for cooperative exploration. *IEEE Transactions on Automatic Control*, 55(3):650–663, 2010.

[61] Tan Zhang, Ning Leng, and Suman Banerjee. A vehicle-based measurement framework for enhancing whitespace spectrum databases. In *Proceedings of the 20th annual international conference on Mobile computing and networking*, pages 17–28. ACM, 2014.

[62] Shengli Zhou and Zhaohui Wang. *OFDM for underwater acoustic communications*. John Wiley & Sons, 2014.